Links between ejecta velocities of supernovae Ia and host galaxy characteristics

L. Barkhudaryan[1], A. Hakobyan[1], A. Karapetyan[1], M. Gevorgyan[1] & V. Adibekyan[2,3]

[1] Center for Cosmology and Astrophysics, Alikhanian National Science Laboratory, Armenia

[2] Instituto de Astrofísica e Ciências do Espaço, Universidade do Porto, CAUP, Portugal

[3] Departamento de Física e Astronomia, Faculdade de Ciências, Universidade do Porto, Portugal

03/04/2025

A. ALIKHANYAN National Laboratory

CURRENT ISSUE

- An asymmetric explosion as the origin of velocity diversity in Type Ia supernovae **?**

- Evidence for (two) distinct populations of Type Ia supernovae **?**

CURRENT ISSUE

- An asymmetric explosion as the origin of velocity diversity in Type Ia supernovae **?**

- Evidence for (two) distinct populations of Type Ia supernovae **?**

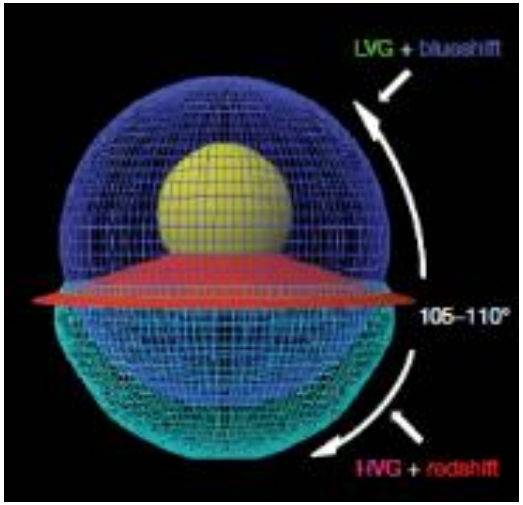

CURRENT ISSUE

- An asymmetric explosion as the origin of velocity diversity in Type Ia supernovae ?

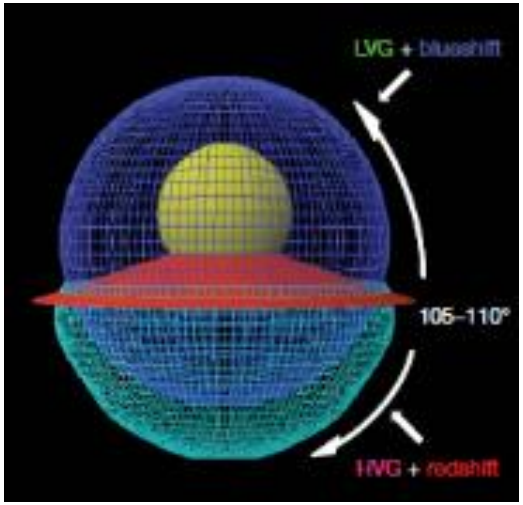

- Evidence for (two) distinct populations of Type Ia supernovae ?

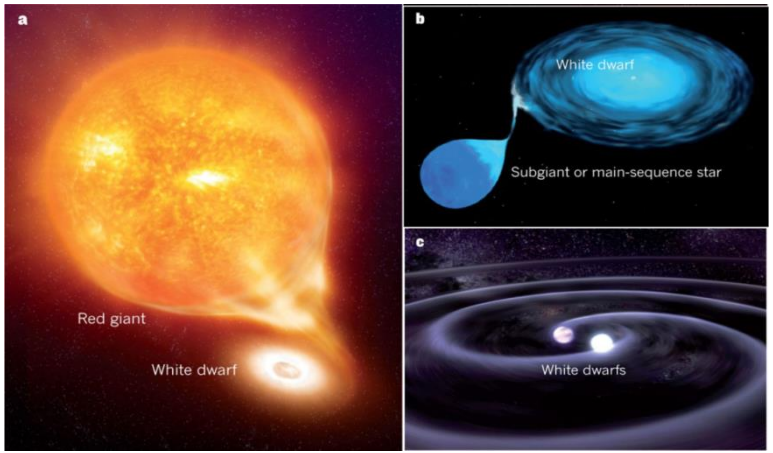

Wang et al. 2013

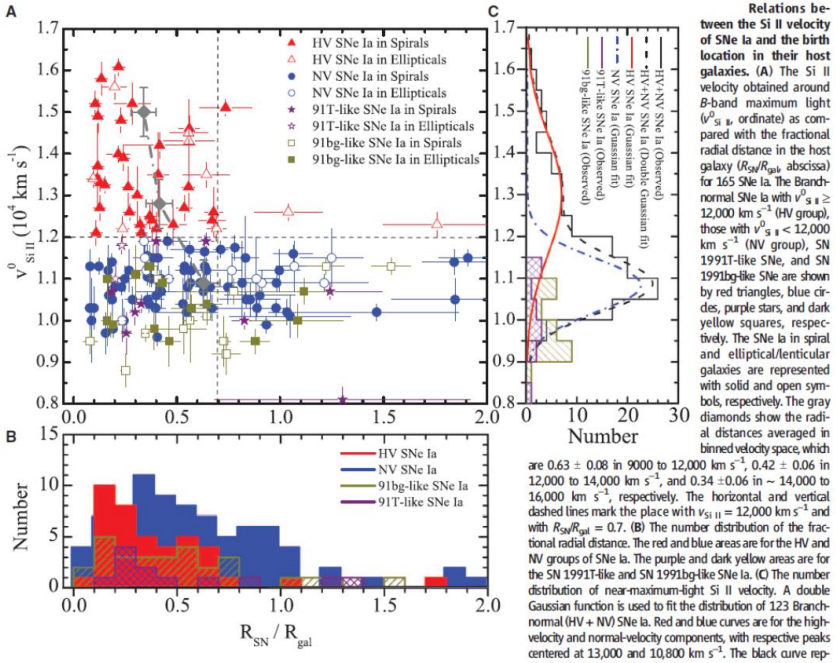

Relations between the Si II velocity of SNe Ia and the birth location in their host galaxies. (**A**) The Si II velocity obtained around *B*-band maximum light ($v^0_{Si\ II}$, ordinate) as compared with the fractional radial distance in the host galaxy (R_{SN}/R_{gal}, abscissa) for 165 SNe Ia. The Branch-normal SNe Ia with $v^0_{Si\ II} \geq$ 12,000 km s^{-1} (HV group), those with $v^0_{Si\ II}$ < 12,000 km s^{-1} (NV group), SN 1991T-like SNe, and SN 1991bg-like SNe are shown by red triangles, blue circles, purple stars, and dark yellow squares, respectively. The SNe Ia in spiral and elliptical/lenticular galaxies are represented with solid and open symbols, respectively. The gray diamonds show the radial distances averaged in binned velocity space, which are 0.63 ± 0.08 in 9000 to 12,000 km s^{-1}, 0.42 ± 0.06 in 12,000 to 14,000 km s^{-1}, and 0.34 ±0.06 in ~ 14,000 to 16,000 km s^{-1}, respectively. The horizontal and vertical dashed lines mark the place with $v_{Si\ II}$ = 12,000 km s^{-1} and with R_{SN}/R_{gal} = 0.7. (**B**) The number distribution of the fractional radial distance. The red and blue areas are for the HV and NV groups of SNe Ia. The purple and dark yellow areas are for the SN 1991T-like and SN 1991bg-like SNe Ia. (**C**) The number distribution of near-maximum-light Si II velocity. A double Gaussian function is used to fit the distribution of 123 Branch-normal (HV + NV) SNe Ia. Red and blue curves are for the high-velocity and normal-velocity components, with respective peaks centered at 13,000 and 10,800 km s^{-1}. The black curve represents the combined result of these two components.

Wang et al. 2013

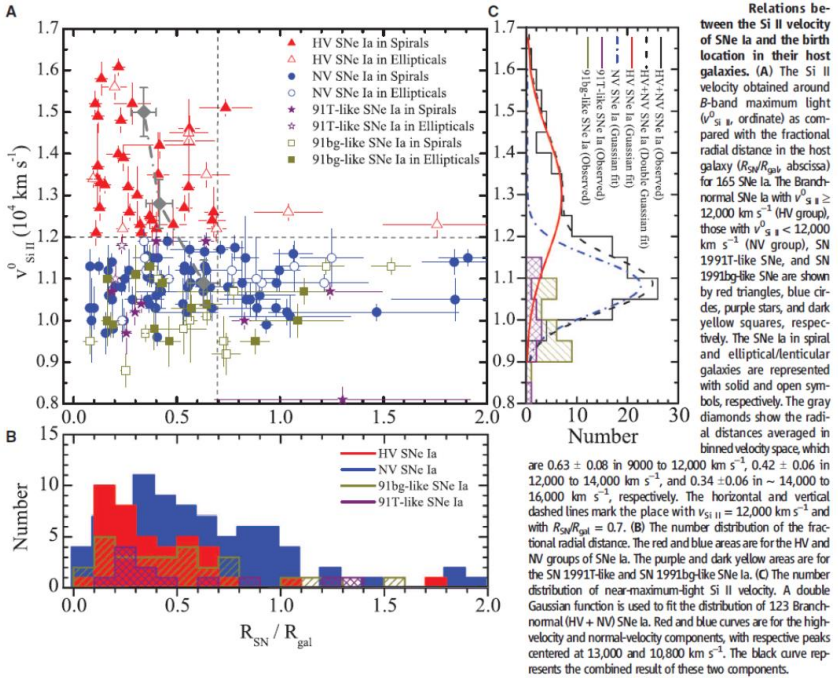

Relations between the Si II velocity of SNe Ia and the birth location in their host galaxies. (**A**) The Si II velocity obtained around *B*-band maximum light ($v^0_{Si\ II}$, ordinate) as compared with the fractional radial distance in the host galaxy (R_{SN}/R_{gal}, abscissa) for 165 SNe Ia. The Branch-normal SNe Ia with $v^0_{Si\ II} \geq$ 12,000 km s^{-1} (HV group), those with $v^0_{Si\ II}$ < 12,000 km s^{-1} (NV group), SN 1991T-like SNe, and SN 1991bg-like SNe are shown by red triangles, blue circles, purple stars, and dark yellow squares, respectively. The SNe Ia in spiral and elliptical/lenticular galaxies are represented with solid and open symbols, respectively. The gray diamonds show the radial distances averaged in binned velocity space, which are 0.63 ± 0.08 in 9000 to 12,000 km s^{-1}, 0.42 ± 0.06 in 12,000 to 14,000 km s^{-1}, and 0.34 ±0.06 in ~ 14,000 to 16,000 km s^{-1}, respectively. The horizontal and vertical dashed lines mark the place with $v_{Si\ II}$ = 12,000 km s^{-1} and with R_{SN}/R_{gal} = 0.7. (**B**) The number distribution of the fractional radial distance. The red and blue areas are for the HV and NV groups of SNe Ia. The purple and dark yellow areas are for the SN 1991T-like and SN 1991bg-like SNe Ia. (**C**) The number distribution of near-maximum-light Si II velocity. A double Gaussian function is used to fit the distribution of 123 Branch-normal (HV + NV) SNe Ia. Red and blue curves are for the high-velocity and normal-velocity components, with respective peaks centered at 13,000 and 10,800 km s^{-1}. The black curve represents the combined result of these two components.

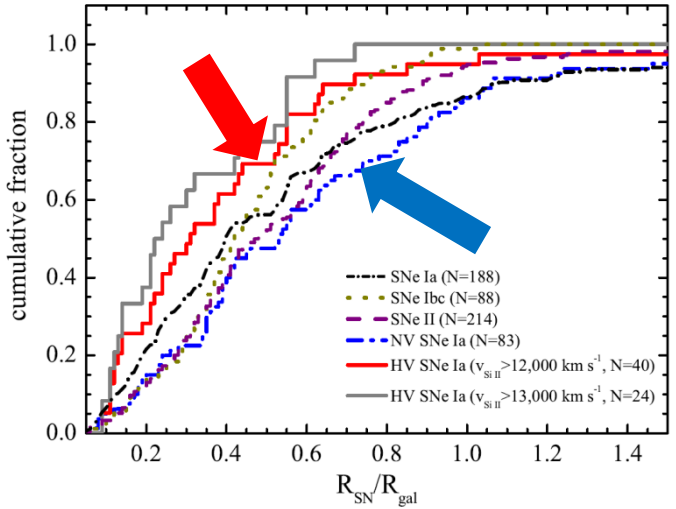

A plot of the cumulative fraction of SN samples

Statistically significant result

Wang et al. 2013

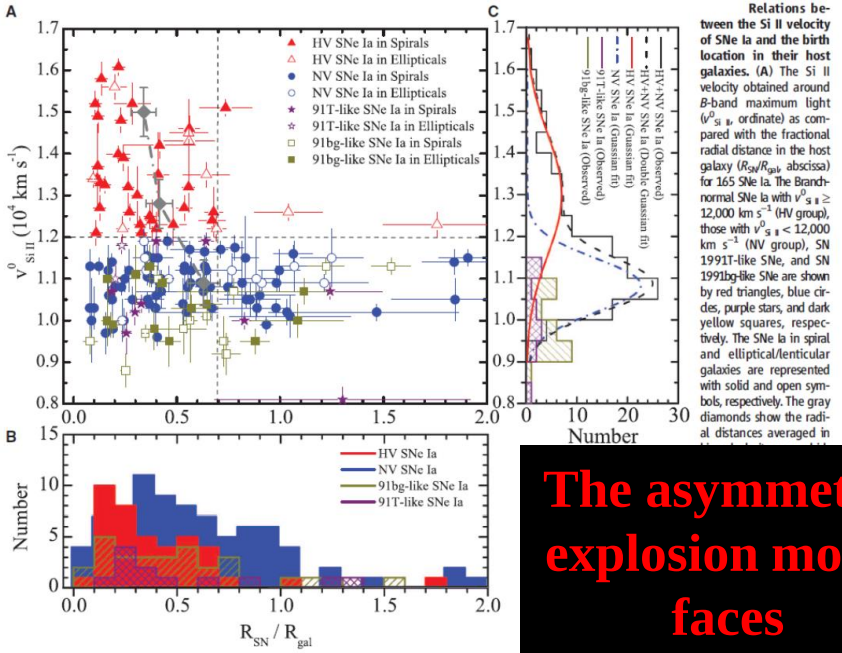

Relations between the Si II velocity of SNe Ia and the birth location in their host galaxies. (**A**) The Si II velocity obtained around *B*-band maximum light ($v^0_{Si\ II}$, ordinate) as compared with the fractional radial distance in the host galaxy (R_{SN}/R_{gal}, abscissa) for 165 SNe Ia. The Branch-normal SNe Ia with $v^0_{Si\ II} \geq$ 12,000 km s^{-1} (HV group), those with $v^0_{Si\ II}$ < 12,000 km s^{-1} (NV group), SN 1991T-like SNe, and SN 1991bg-like SNe are shown by red triangles, blue circles, purple stars, and dark yellow squares, respectively. The SNe Ia in spiral and elliptical/lenticular galaxies are represented with solid and open symbols, respectively. The gray diamonds show the radial distances averaged in

The asymmetric explosion model faces complications

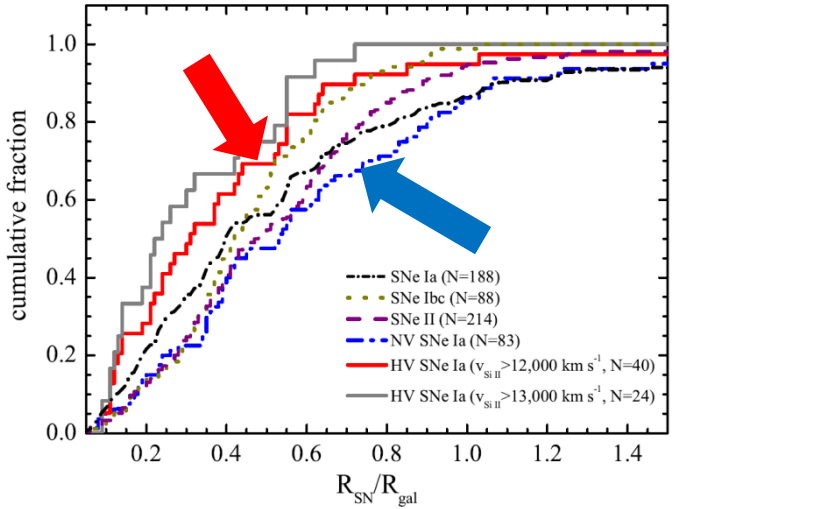

A plot of the cumulative fraction of SN samples

Statistically significant result

Wang et al. 2013

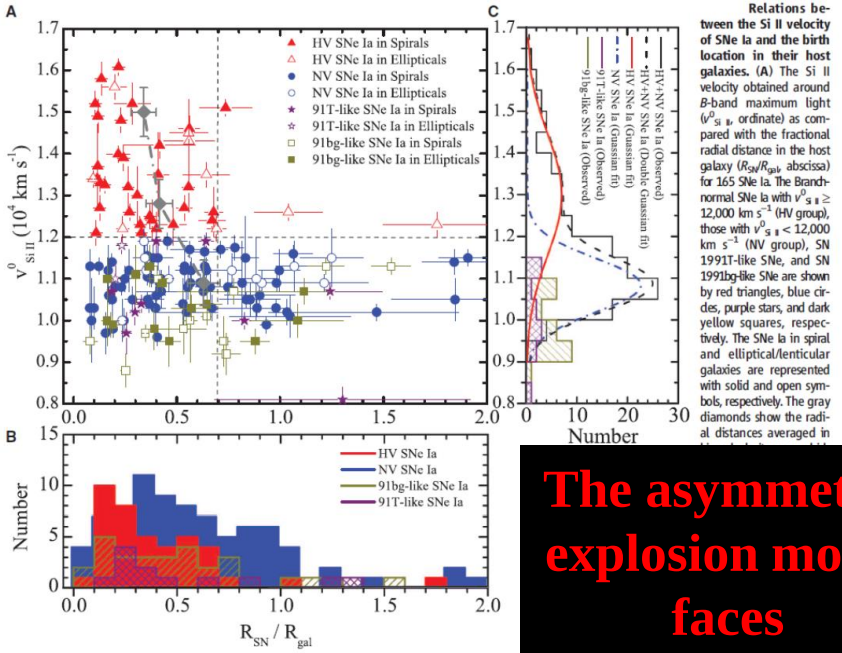

Relations between the Si II velocity of SNe Ia and the birth location in their host galaxies. (**A**) The Si II velocity obtained around *B*-band maximum light ($v^0_{Si\ II}$, ordinate) as compared with the fractional radial distance in the host galaxy (R_{SN}/R_{gal}, abscissa) for 165 SNe Ia. The Branch-normal SNe Ia with $v^0_{Si\ II} \geq$ 12,000 km s^{-1} (HV group), those with $v^0_{Si\ II}$ < 12,000 km s^{-1} (NV group), SN 1991T-like SNe, and SN 1991bg-like SNe are shown by red triangles, blue circles, purple stars, and dark yellow squares, respectively. The SNe Ia in spiral and elliptical/lenticular galaxies are represented with solid and open symbols, respectively. The gray diamonds show the radial distances averaged in

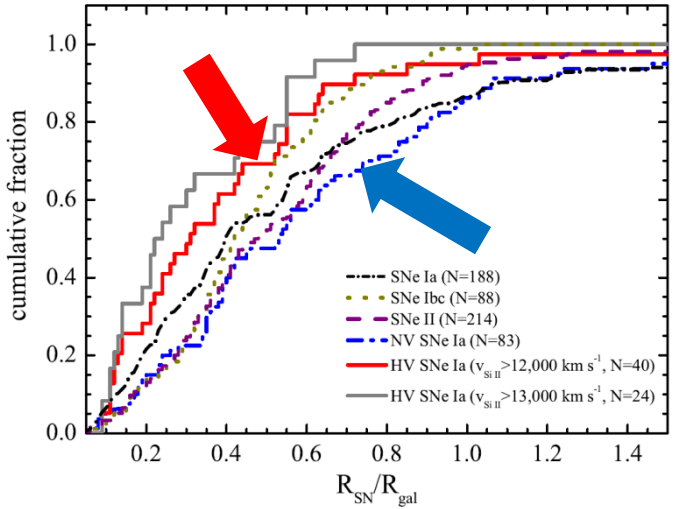

A plot of the cumulative fraction of SN samples

The asymmetric explosion model faces complications

NV SNe

Statistically significant result

Entire galactic disc

Wang et al. 2013

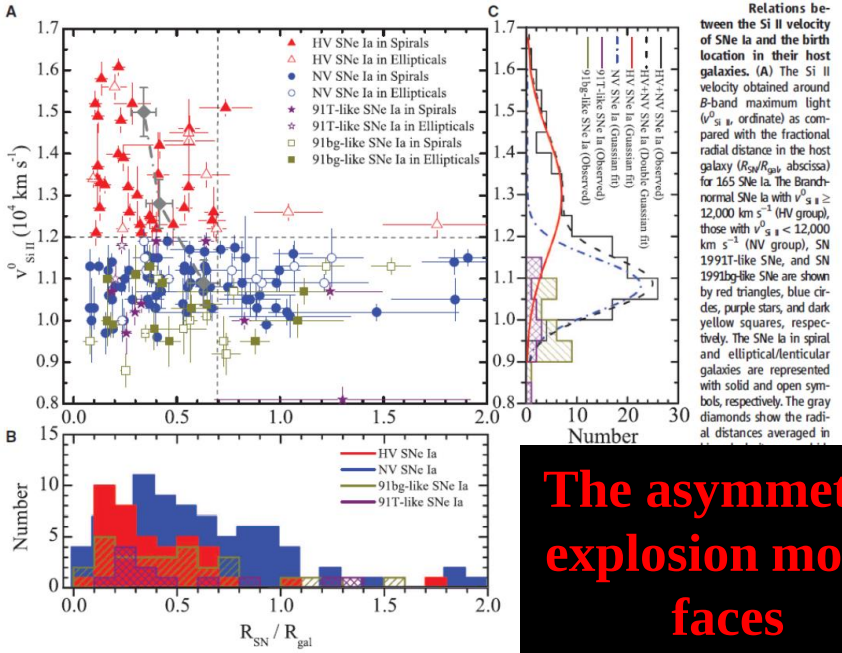

Relations between the Si II velocity of SNe Ia and the birth location in their host galaxies. (**A**) The Si II velocity obtained around *B*-band maximum light ($v^0_{Si\ II}$, ordinate) as compared with the fractional radial distance in the host galaxy (R_{SN}/R_{gal}, abscissa) for 165 SNe Ia. The Branch-normal SNe Ia with $v^0_{Si\ II} \geq$ 12,000 km s^{-1} (HV group), those with $v^0_{Si\ II}$ < 12,000 km s^{-1} (NV group), SN 1991T-like SNe, and SN 1991bg-like SNe are shown by red triangles, blue circles, purple stars, and dark yellow squares, respectively. The SNe Ia in spiral and elliptical/lenticular galaxies are represented with solid and open symbols, respectively. The gray diamonds show the radial distances averaged in

The asymmetric explosion model faces complications

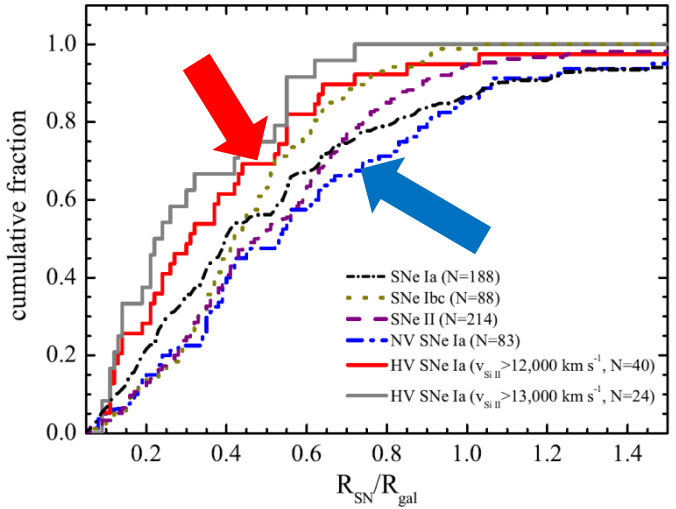

A plot of the cumulative fraction of SN samples

Statistically significant result

NV SNe

Entire galactic disc

HV SNe

Inner and brighter regions

Wang et al. 2013

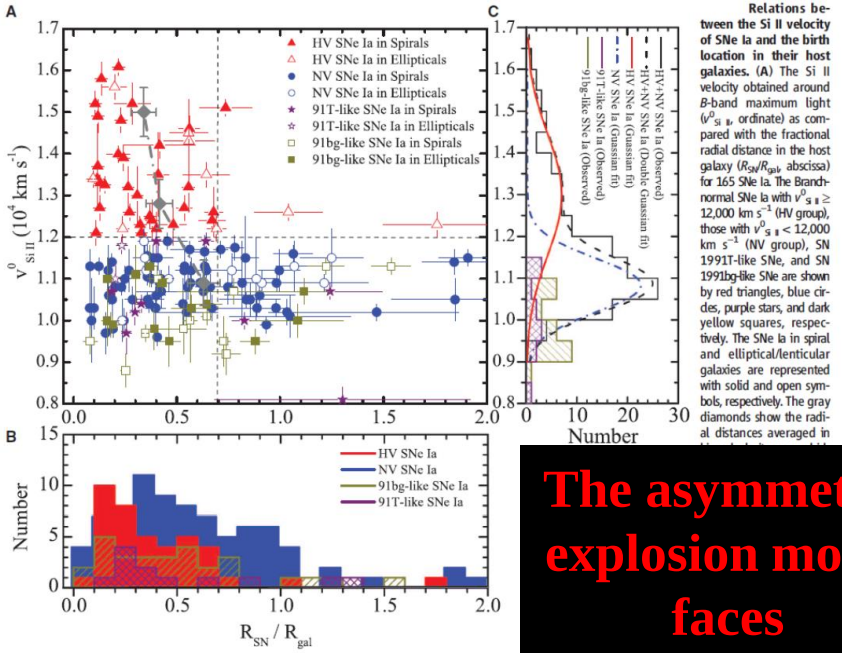

Relations between the Si II velocity of SNe Ia and the birth location in their host galaxies. (**A**) The Si II velocity obtained around *B*-band maximum light ($v^0_{Si\ II}$, ordinate) as compared with the fractional radial distance in the host galaxy (R_{SN}/R_{gal}, abscissa) for 165 SNe Ia. The Branch-normal SNe Ia with $v^0_{Si\ II} \geq$ 12,000 km s^{-1} (HV group), those with $v^0_{Si\ II}$ < 12,000 km s^{-1} (NV group), SN 1991T-like SNe, and SN 1991bg-like SNe are shown by red triangles, blue circles, purple stars, and dark yellow squares, respectively. The SNe Ia in spiral and elliptical/lenticular galaxies are represented with solid and open symbols, respectively. The gray diamonds show the radial distances averaged in

The asymmetric explosion model faces complications

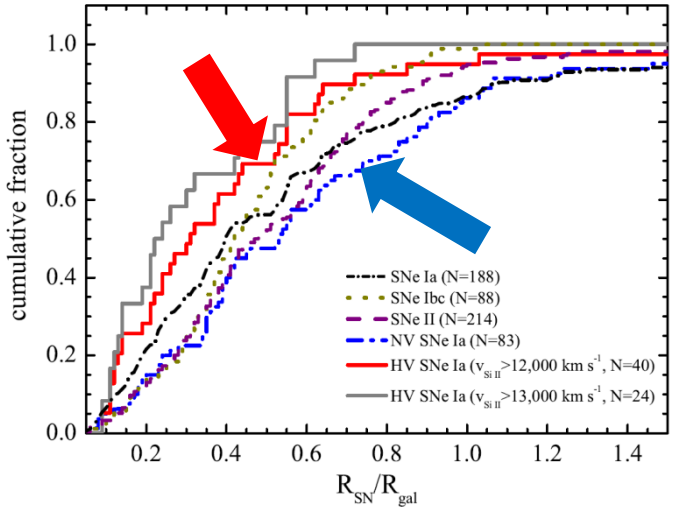

A plot of the cumulative fraction of SN samples

Statistically significant result

NV SNe → **Entire galactic disc**

HV SNe → **Inner and brighter regions** → **metal rich (younger) progenitors**

The Si II λ6355 velocities ($v_{\mathrm{Si\,II}}$) as a function of $R_{\mathrm{SN}}/R_{\mathrm{gal}}$

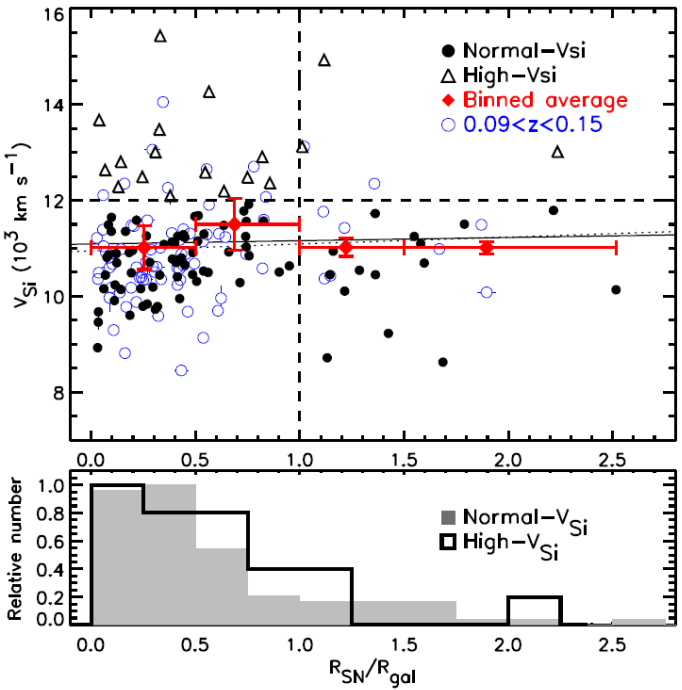

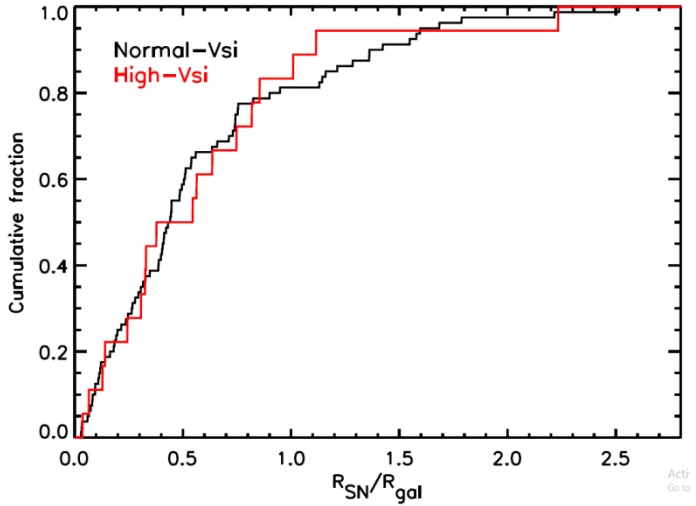

Pan et al. 2015

The Si II λ6355 velocities ($v_{\mathrm{Si\,II}}$) as a function of $R_{\mathrm{SN}}/R_{\mathrm{gal}}$

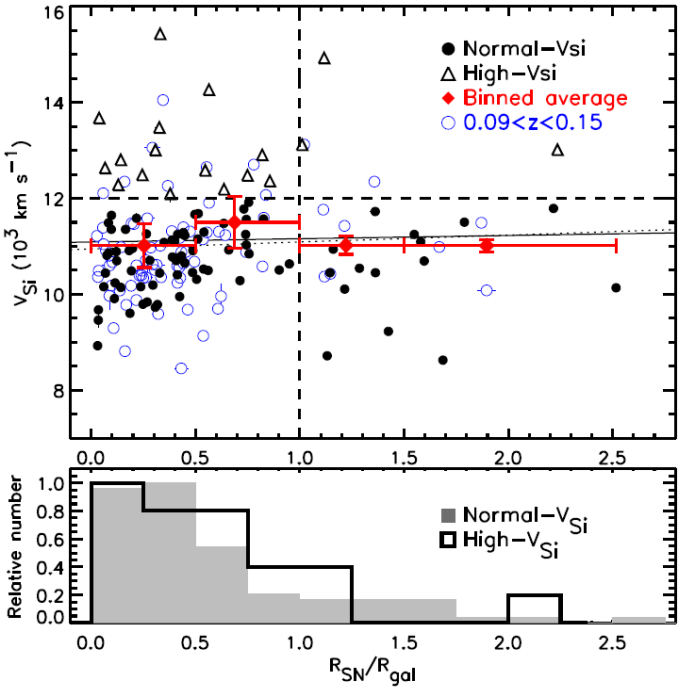

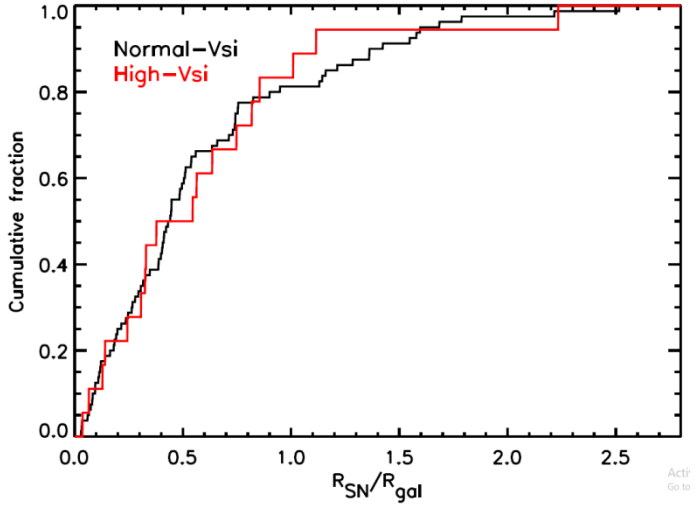

Statistically <u>not</u> significant result

Pan et al. 2015

The Si II λ6355 velocities ($v_{\mathrm{Si\,II}}$) as a function of $R_{\mathrm{SN}}/R_{\mathrm{gal}}$

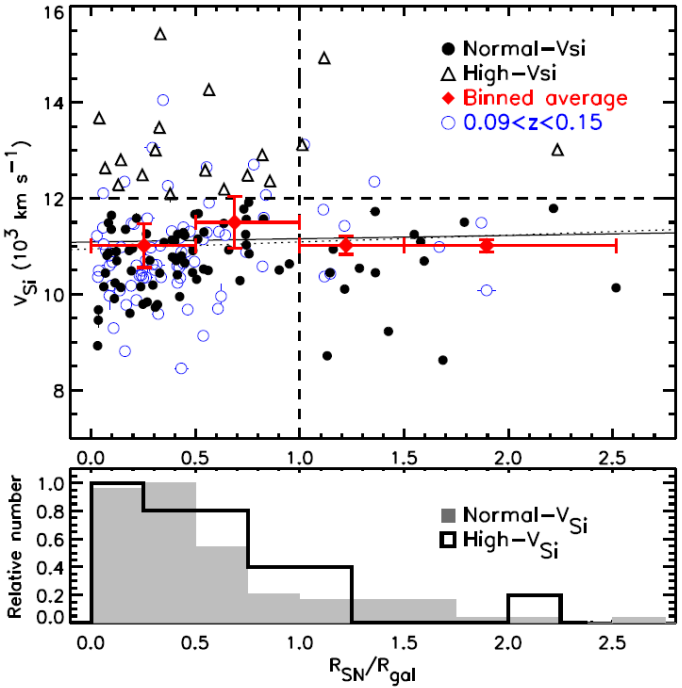

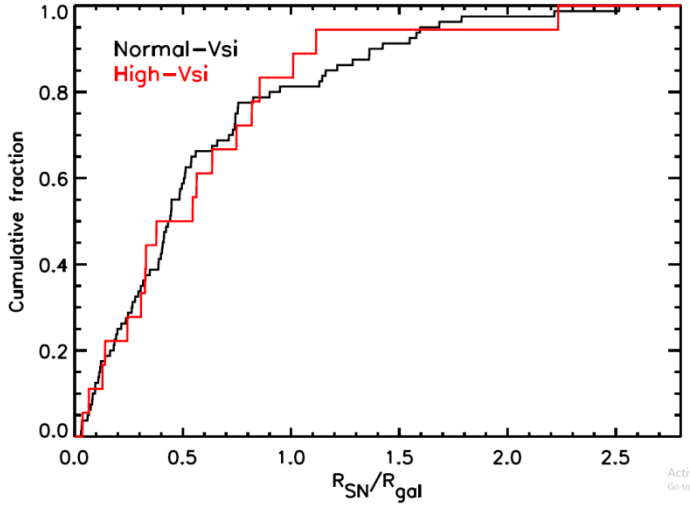

Statistically <u>not</u> significant result

Pan et al. 2015

The same interpretation of the result

Si II λ6355 velocities ($v_{\mathrm{Si\ II}}$) as a function of host-galaxy stellar mass (M_{stellar}).

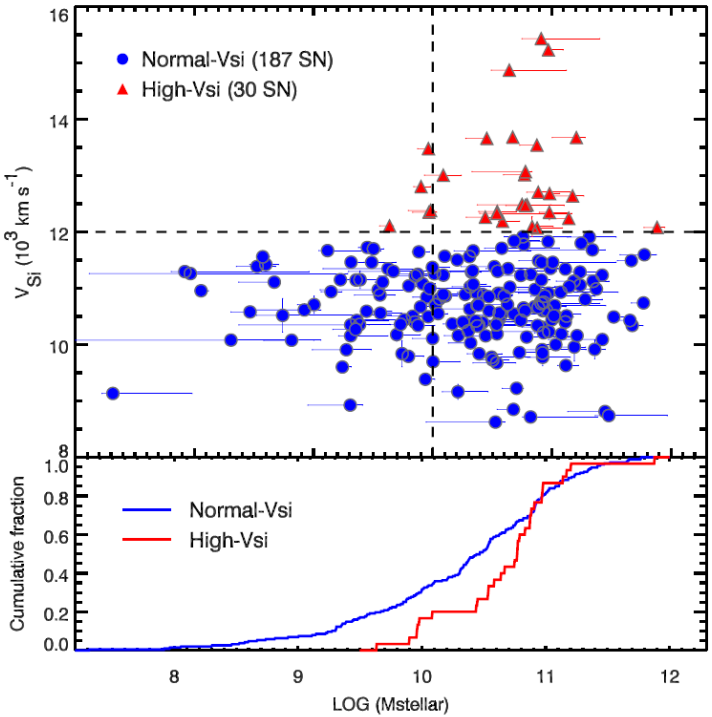

Pan 2020

Si II λ6355 velocities ($v_{\mathrm{Si\ II}}$) as a function of host-galaxy stellar mass (M_{stellar}).

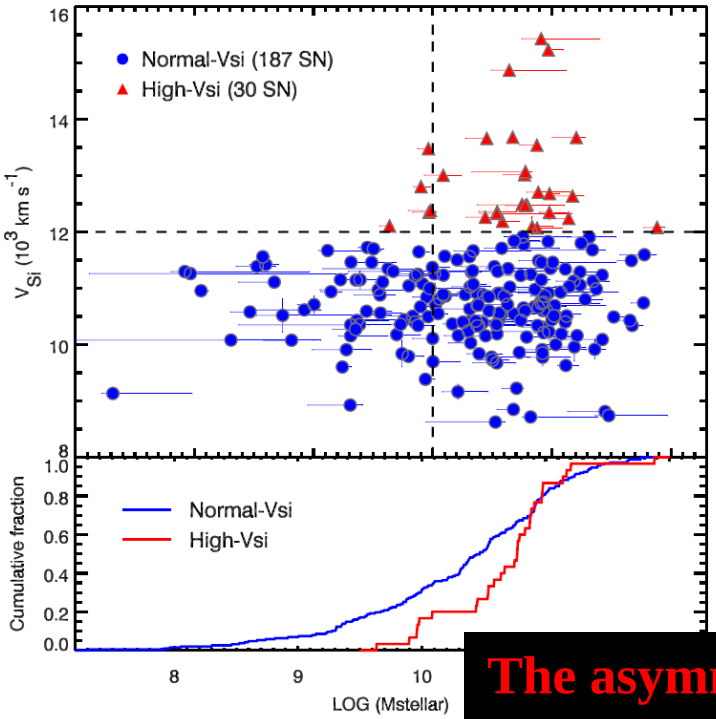

Pan 2020

The asymmetric explosion model faces complications

Si II λ6355 velocities ($v_{\mathrm{Si\ II}}$) as a function of host-galaxy stellar mass (M_{stellar}).

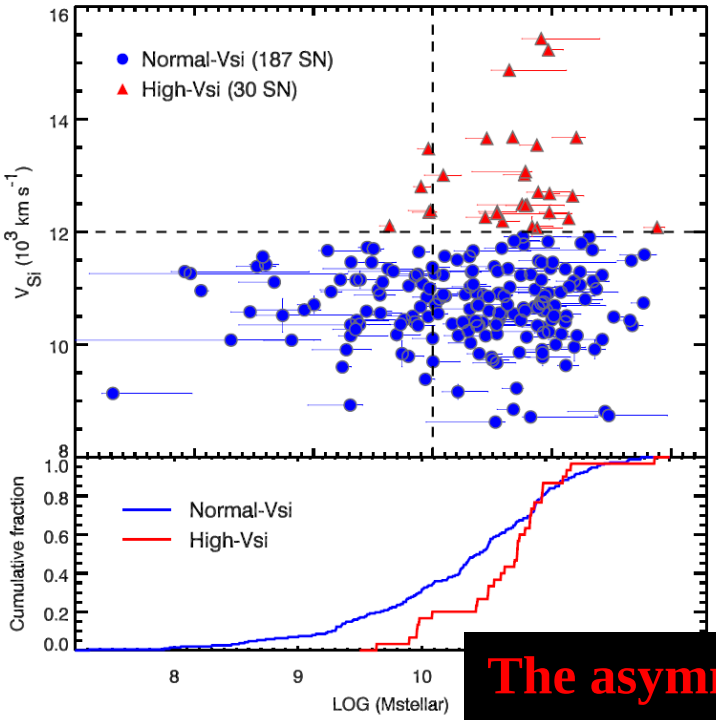

Pan 2020

The asymmetric explosion model faces complications

NV SNe

All masses

Si II λ6355 velocities ($v_{\mathrm{Si\ II}}$) as a function of host-galaxy stellar mass (M_{stellar}).

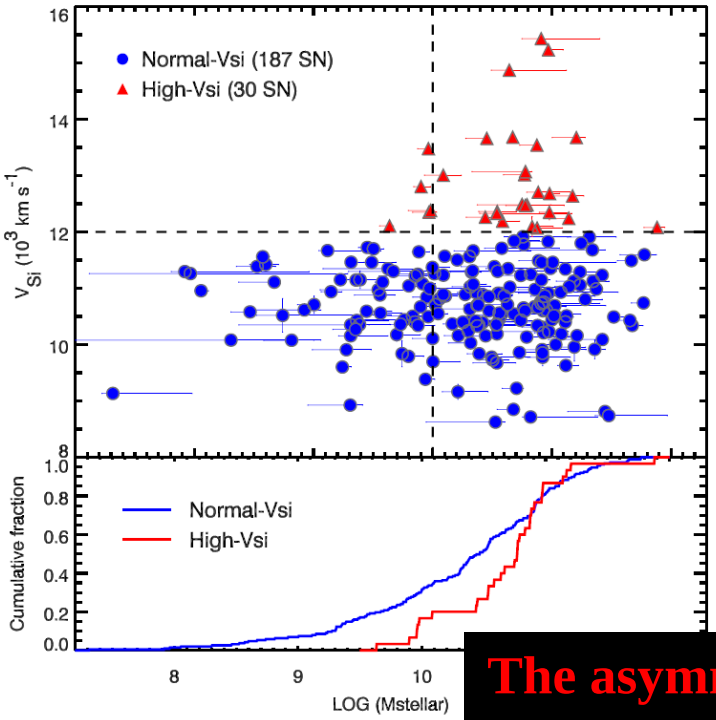

Pan 2020

The asymmetric explosion model faces complications

NV SNe

All masses

HV SNe

High mass

Si II λ6355 velocities ($v_{\mathrm{Si\ II}}$) as a function of host-galaxy stellar mass (M_{stellar}).

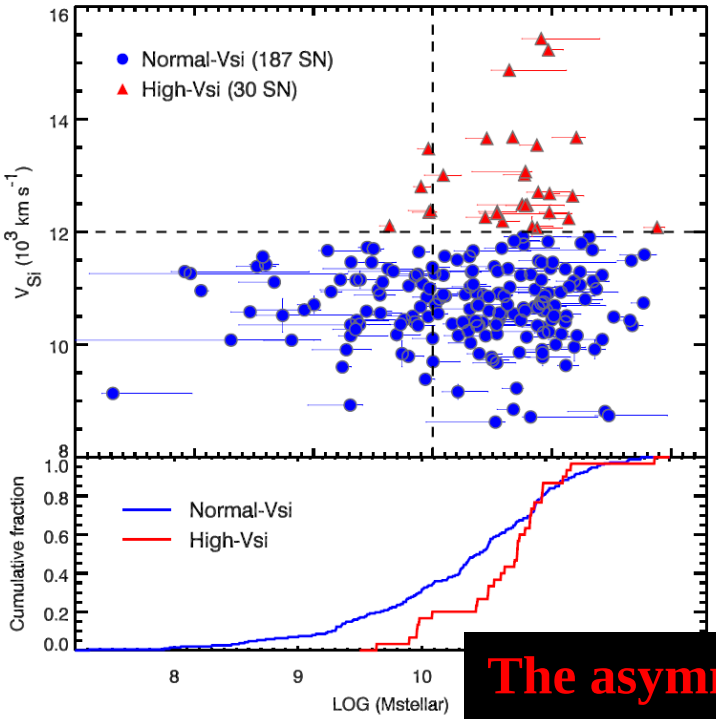

Pan 2020

The asymmetric explosion model faces complications

NV SNe

All masses

HV SNe

High mass

metal rich progenitors

Si II λ6355 velocities ($v_{\mathrm{Si\ II}}$) as a function of host-galaxy stellar mass (M_{stellar}).

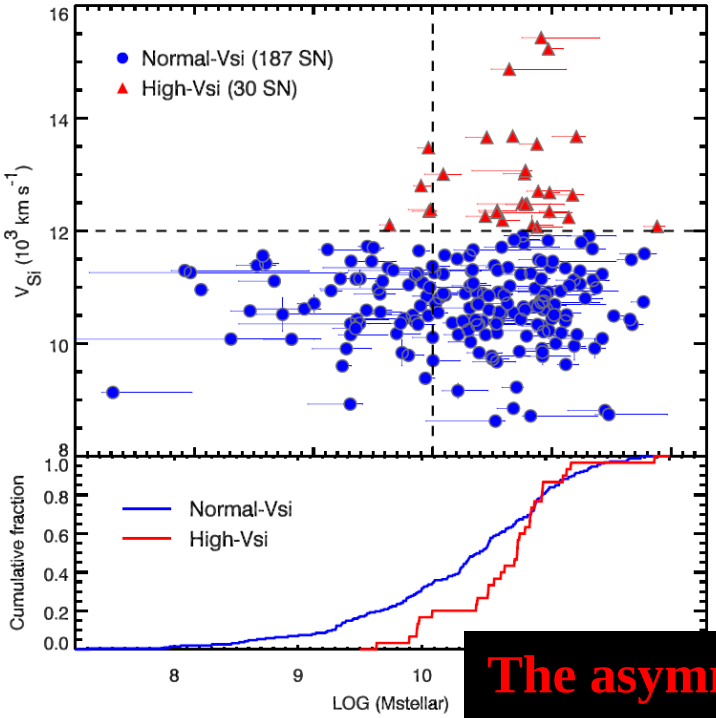

Pan 2020

The asymmetric explosion model faces complications

Si II λ6355 velocities ($v_{\mathrm{Si\ II}}$) as a function of redshift.

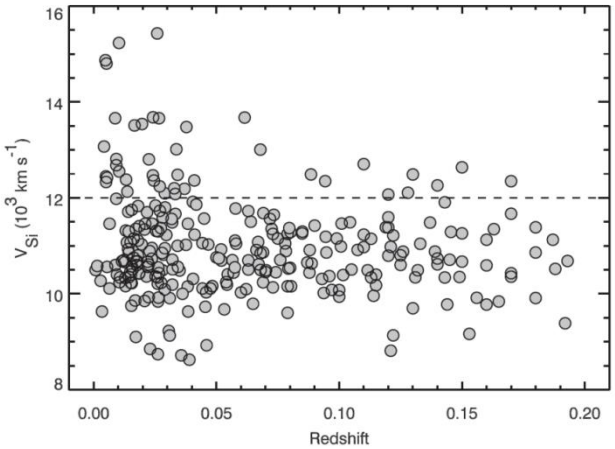

NV SNe → **All masses**

HV SNe → **High mass** → **metal rich progenitors**

Si II λ6355 velocities ($v_{\mathrm{Si\ II}}$) as a function of host-galaxy stellar mass (M_{stellar}).

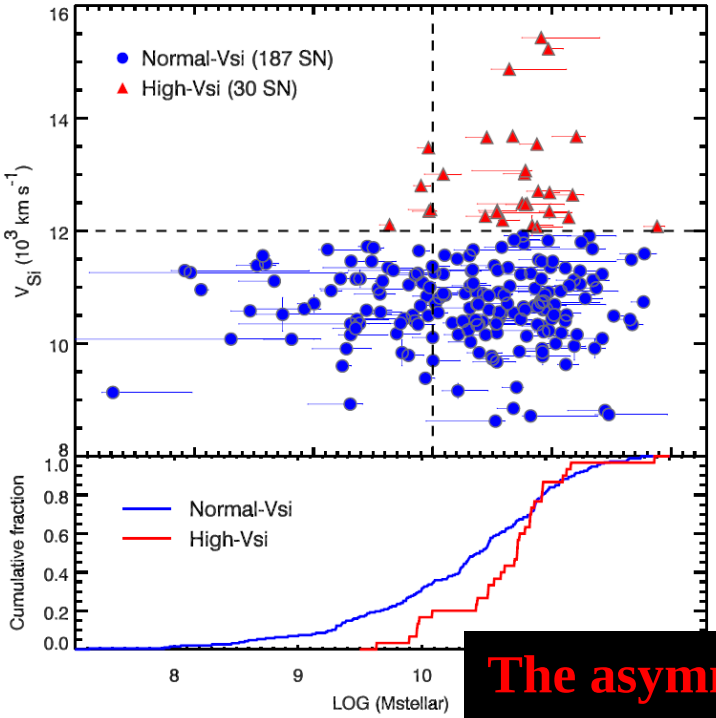

Pan 2020

The asymmetric explosion model faces complications

Si II λ6355 velocities ($v_{\mathrm{Si\ II}}$) as a function of redshift.

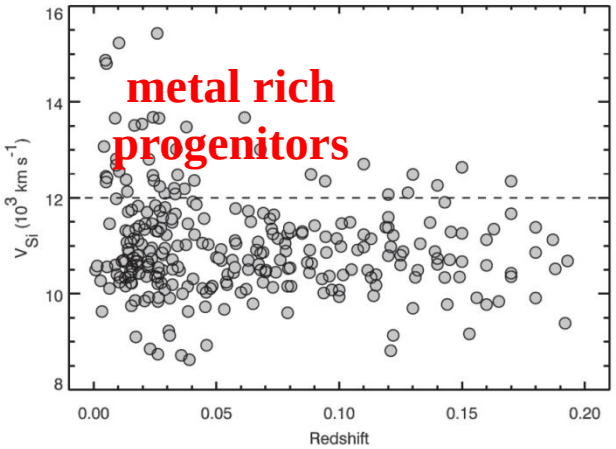

NV SNe → **All masses**

HV SNe → **High mass** → **metal rich progenitors**

Wang et al. 2013
Sample

- 83 NV and 40 HV Supernovae Ia
- $\boldsymbol{R_{SN}}$ normalized to the $\boldsymbol{R_{25} = D_{25}/2}$ to bring the galaxies in this study to relatively the same size
- the morphologies are Ellipticals, Spirals with $0° \leq i \leq 90°$ inclinations
- Inclination corrections done for Spirals with $0° \leq i \leq 70°$

Wang et al. 2013 Sample

- 83 NV and 40 HV Supernovae Ia
- $\boldsymbol{R_{SN}}$ normalized to the $\boldsymbol{R_{25} = D_{25}/2}$ to bring the galaxies in this study to relatively the same size
- the morphologies are Ellipticals, Spirals with $0° \leq i \leq 90°$ inclinations
- Inclination corrections done for Spirals with $0° \leq i \leq 70°$

Pan 2020 Sample

- 122 Supernovae Ia
- $\boldsymbol{R_{SN}}$ normalized to the $\boldsymbol{R_{gal}}$, defined as the radius at which 90 per cent of the flux from the galaxy is enclosed
- the morphologies are E, S0, Sa, Sb, Sbc, Sc, Sd, Im with $0° \leq i \leq 90°$ inclinations
- no deprojection is applied for the host galaxies

Wang et al. 2013 Sample

- 83 NV and 40 HV Supernovae Ia
- R_{SN} normalized to the $R_{25} = D_{25}/2$ to bring the galaxies in this study to relatively the same size
- the morphologies are Ellipticals, Spirals with $0° \leq i \leq 90°$ inclinations
- Inclination corrections done for Spirals with $0° \leq i \leq 70°$

Pan 2020 Sample

- 122 Supernovae Ia
- R_{SN} normalized to the R_{gal}, defined as the radius at which 90 per cent of the flux from the galaxy is enclosed
- the morphologies are E, S0, Sa, Sb, Sbc, Sc, Sd, Im with $0° \leq i \leq 90°$ inclinations
- no deprojection is applied for the host galaxies

Barkhudaryan et al. 2025 Our sample

- Spectroscopically classified 397 Type Ia SNe
- Entire sky (SDSS, Pan-STARRS, and SkyMapper Survey)
- the morphologies are E - S0 - Sd types with $0° \leq i \leq 90°$ inclinations.
- any galaxy exhibiting strong disturbances are excluded
- Redshifts $z \leq 0.04$

We use the **$R_{25} = D_{25}/2$ normalization** to bring the galaxies in this study to relatively the same size.

Also, we apply inclination correction for spiral galaxies with $0° \leq i \leq 70°$ inclinations.

Wang sample

Ellipticals

Lenticulars

face-on Spirals

Irregulars

interacting

merging

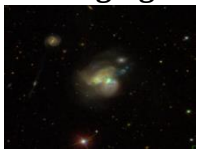

edge-on Spirals

Wang sample

Projected (E) + deprojected (L & S)

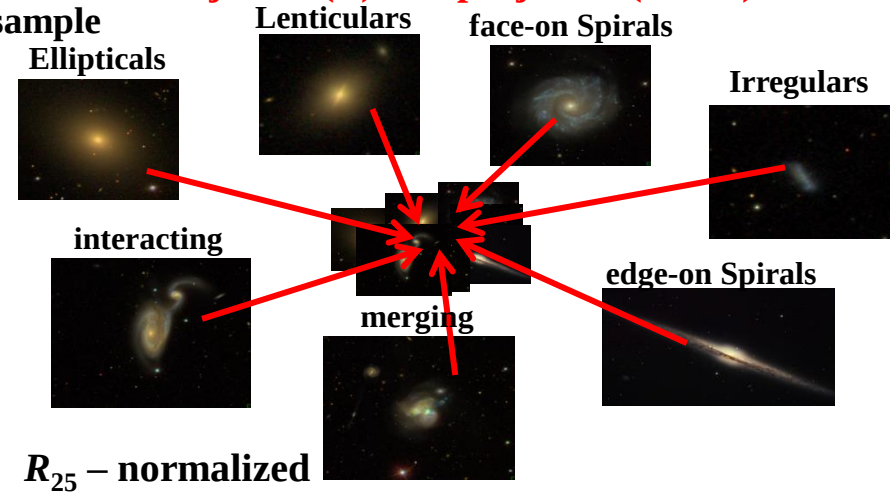

R_{25} – normalized

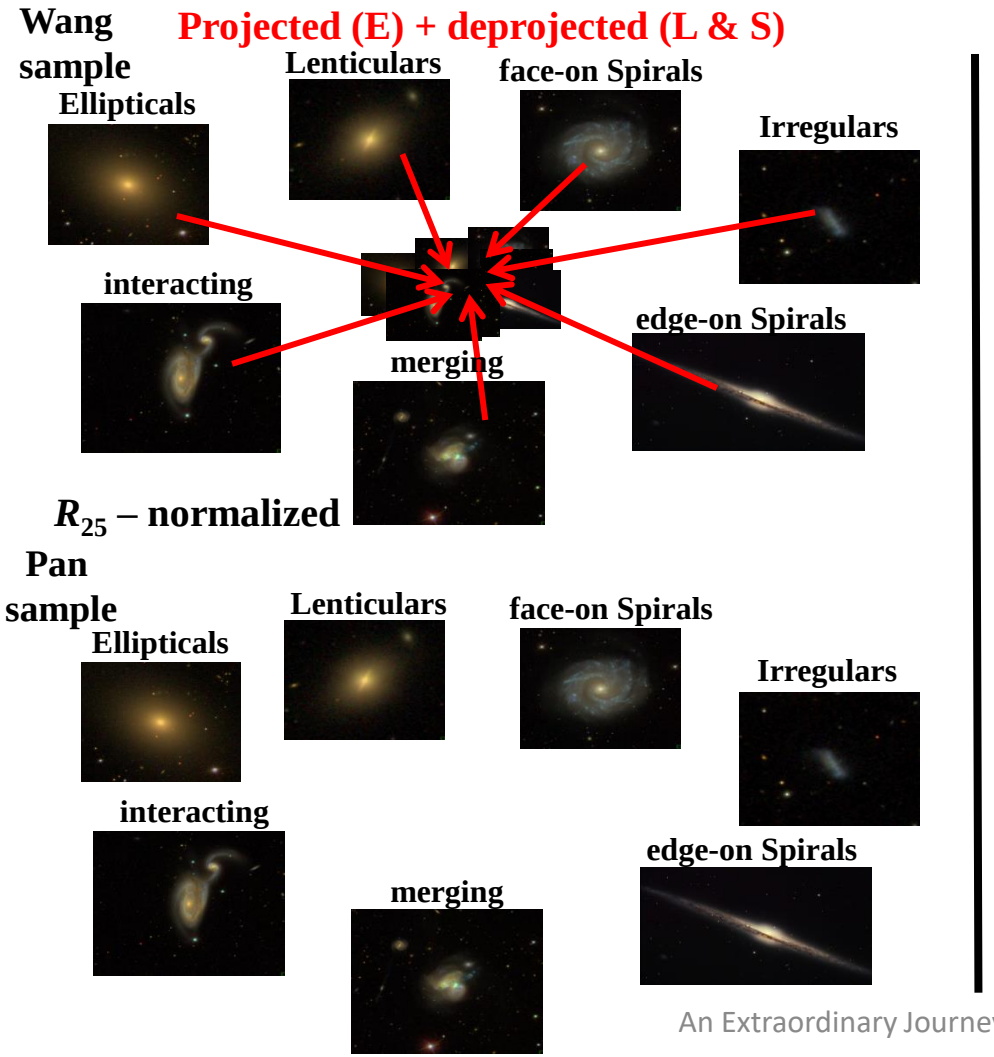
Wang sample
Projected (E) + deprojected (L & S)
Ellipticals
Lenticulars
face-on Spirals
Irregulars
interacting
merging
edge-on Spirals
R_{25} – normalized
Pan sample
Ellipticals
Lenticulars
face-on Spirals
Irregulars
interacting
merging
edge-on Spirals

Wang sample

Projected (E) + deprojected (L & S)

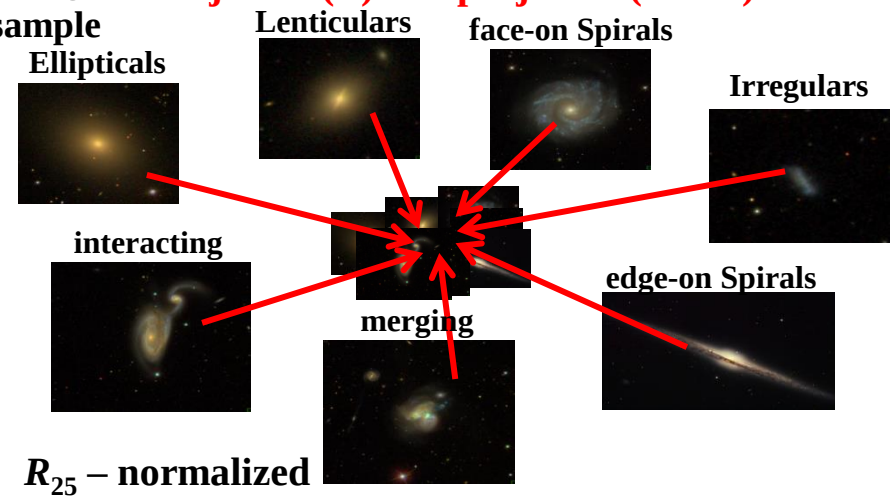

R_{25} – normalized

Pan sample

projected

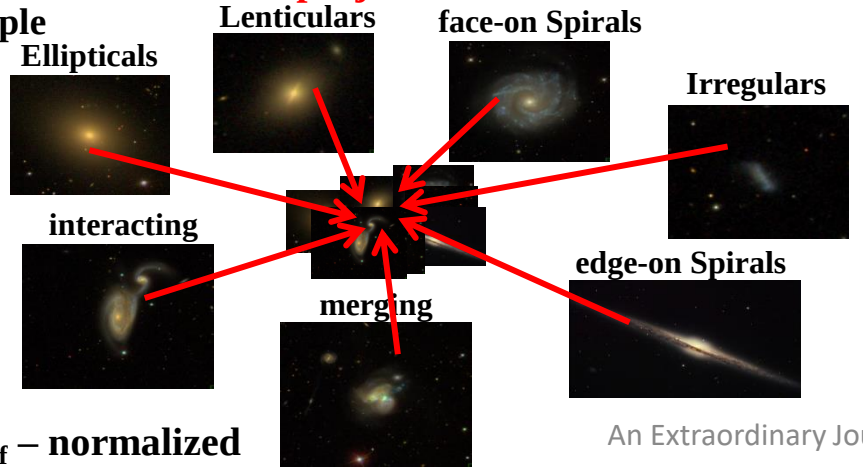

R_{eff} – normalized

Wang sample

Projected (E) + deprojected (L & S)

Ellipticals

Lenticulars

face-on Spirals

Irregulars

interacting

edge-on Spirals

merging

R_{25} – normalized

Pan sample

projected

Ellipticals

Lenticulars

face-on Spirals

Irregulars

interacting

edge-on Spirals

merging

R_{eff} – normalized

Our sample

Ellipticals

Lenticulars

face-on Spirals

Irregulars

edge-on Spirals

interacting

merging

Wang sample

Projected (E) + deprojected (L & S)

Ellipticals

Lenticulars

face-on Spirals

Irregulars

interacting

merging

edge-on Spirals

R_{25} – normalized

Pan sample

projected

Ellipticals

Lenticulars

face-on Spirals

Irregulars

interacting

merging

edge-on Spirals

R_{eff} – normalized

Our sample

projected

Ellipticals

complicated

Lenticulars

deprojected

face-on Spirals

Irregulars

edge-on Spirals

interacting

merging

R_{25} – normalized

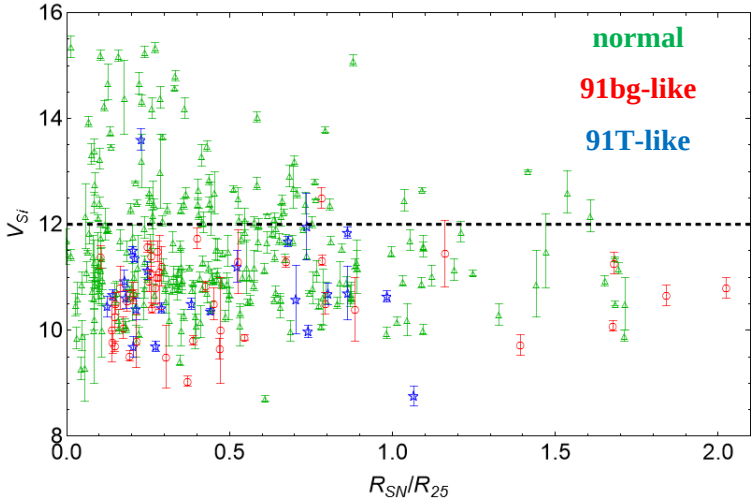
normal
91bg-like
91T-like
V_{Si}
R_{SN}/R_{25}
16
14
12
10
8
0.0
0.5
1.0
1.5
2.0

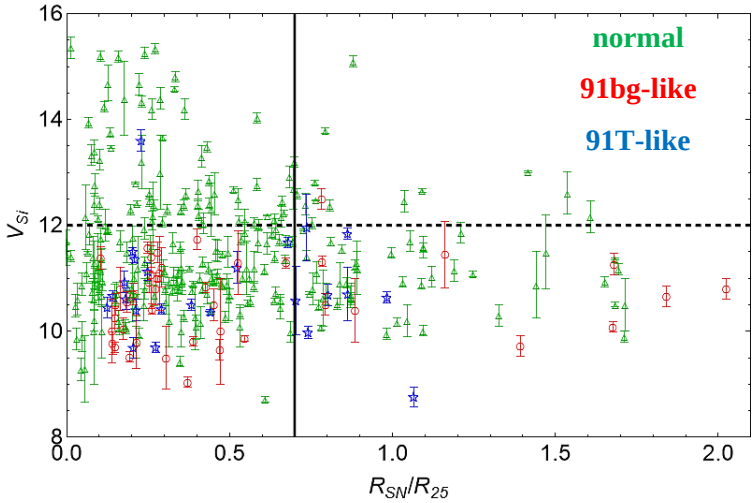
normal
91bg-like
91T-like
V_{Si}
R_{SN}/R_{25}

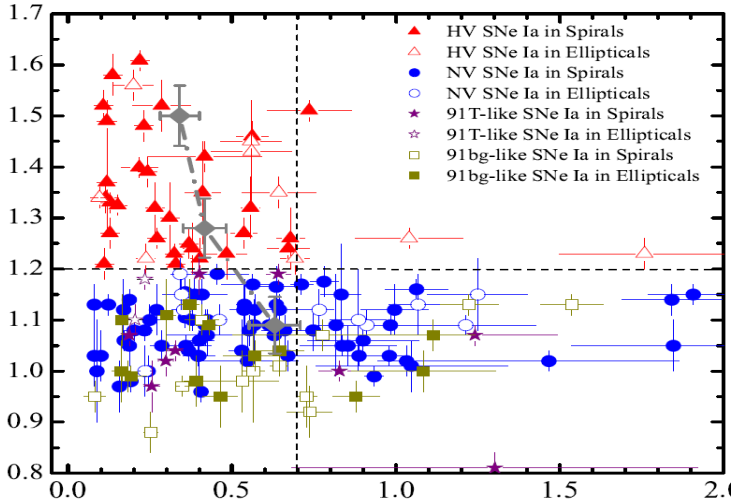
HV SNe Ia in Spirals
HV SNe Ia in Ellipticals
NV SNe Ia in Spirals
NV SNe Ia in Ellipticals
91T-like SNe Ia in Spirals
91T-like SNe Ia in Ellipticals
91bg-like SNe Ia in Spirals
91bg-like SNe Ia in Ellipticals

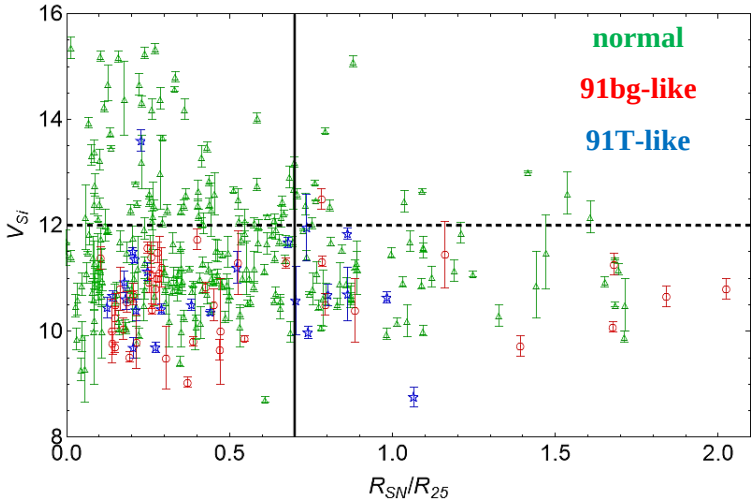
normal
91bg-like
91T-like
v_{Si}
R_{SN}/R_{25}

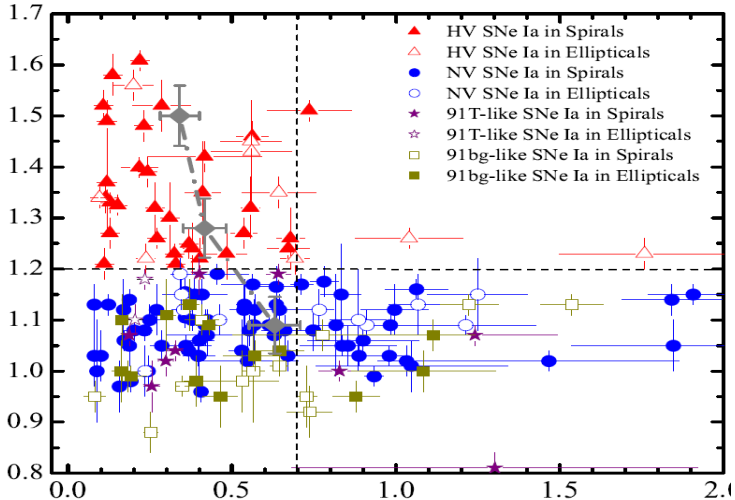
HV SNe Ia in Spirals
HV SNe Ia in Ellipticals
NV SNe Ia in Spirals
NV SNe Ia in Ellipticals
91T-like SNe Ia in Spirals
91T-like SNe Ia in Ellipticals
91bg-like SNe Ia in Spirals
91bg-like SNe Ia in Ellipticals

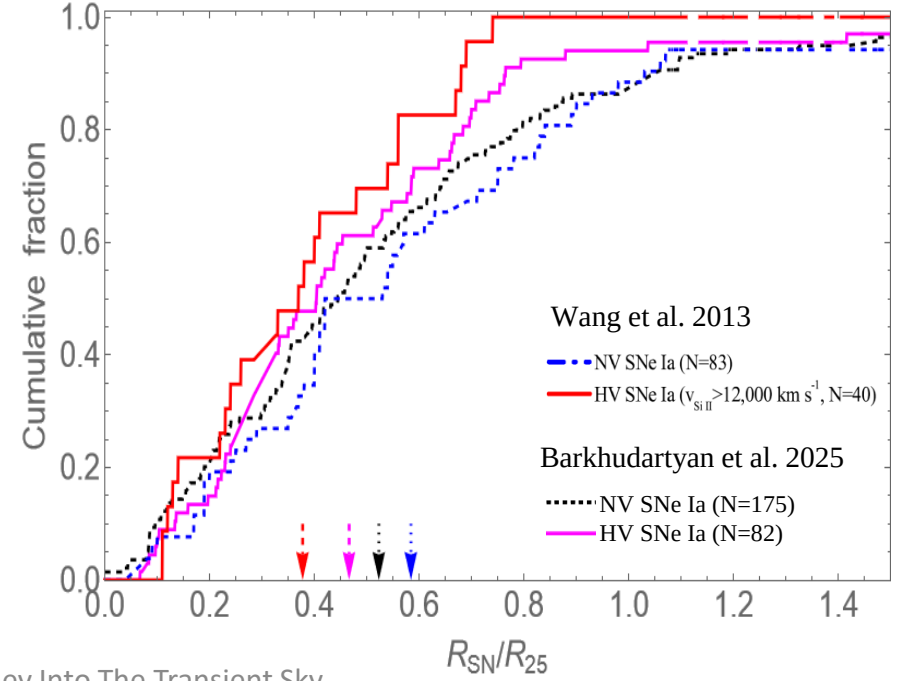
Cumulative fraction
Wang et al. 2013
NV SNe Ia (N=83)
HV SNe Ia ($v_{Si\,II}$>12,000 km s^{-1}, N=40)
Barkhudartyan et al. 2025
NV SNe Ia (N=175)
HV SNe Ia (N=82)
R_{SN}/R_{25}

Statistically not significant result

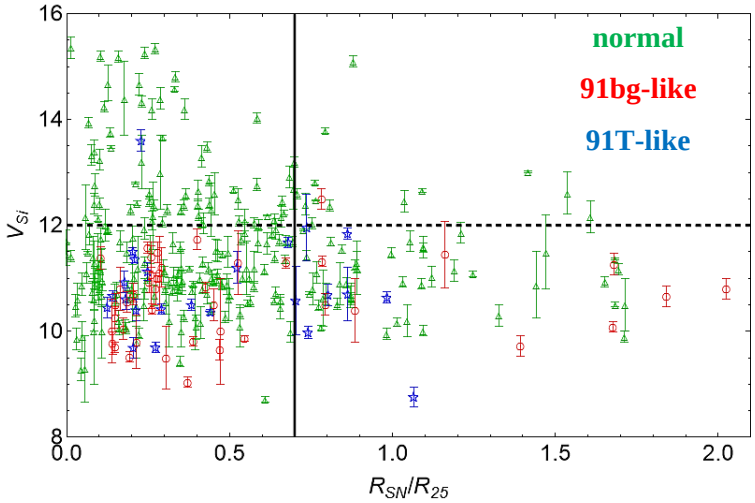

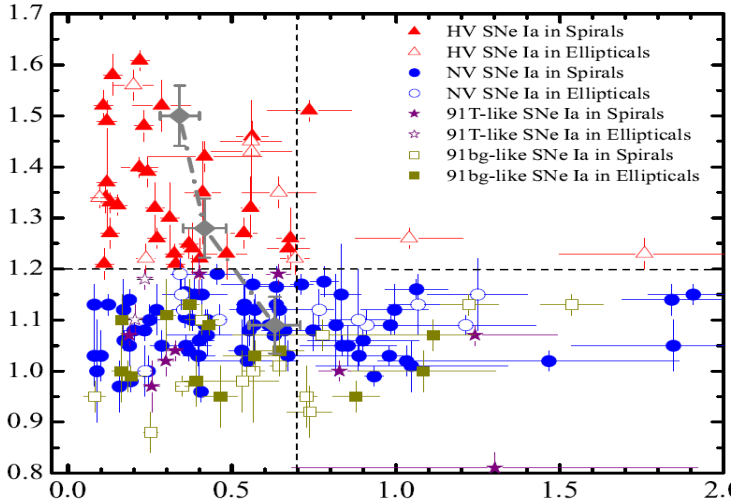

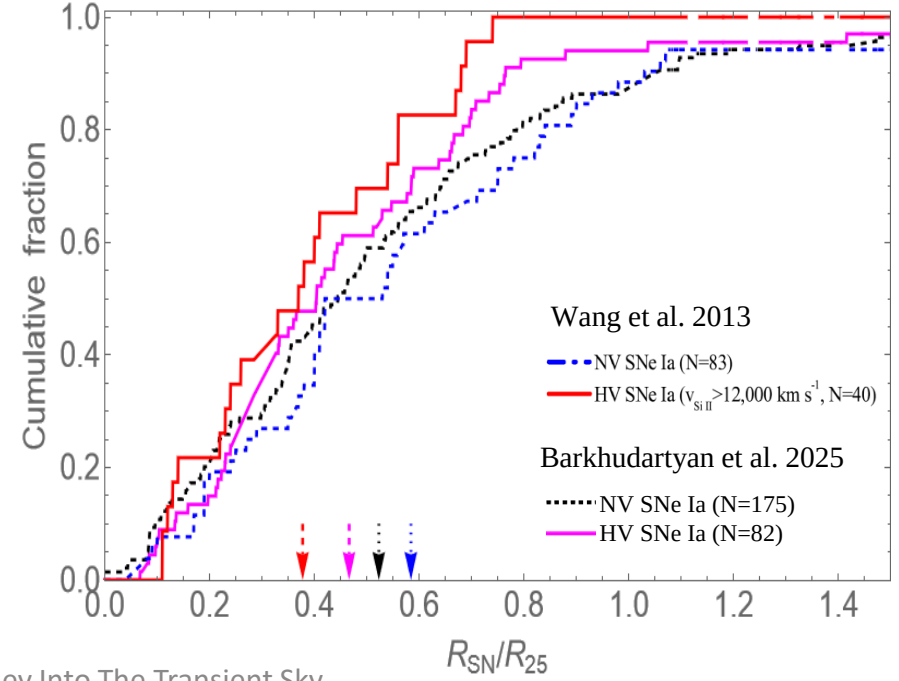

Statistically not significant result

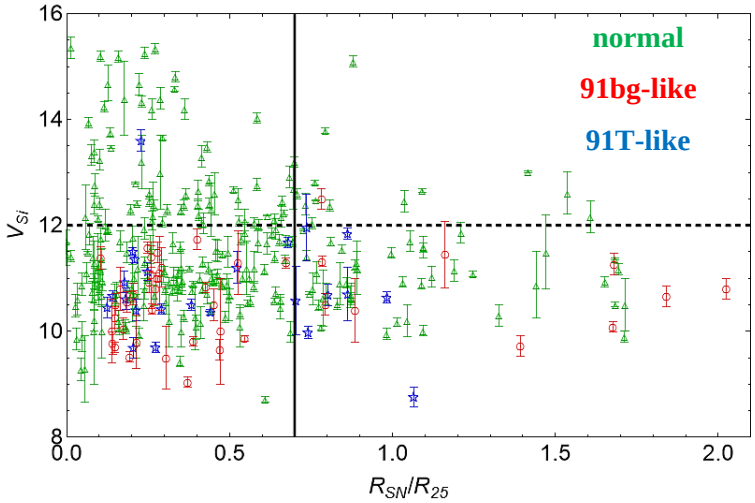

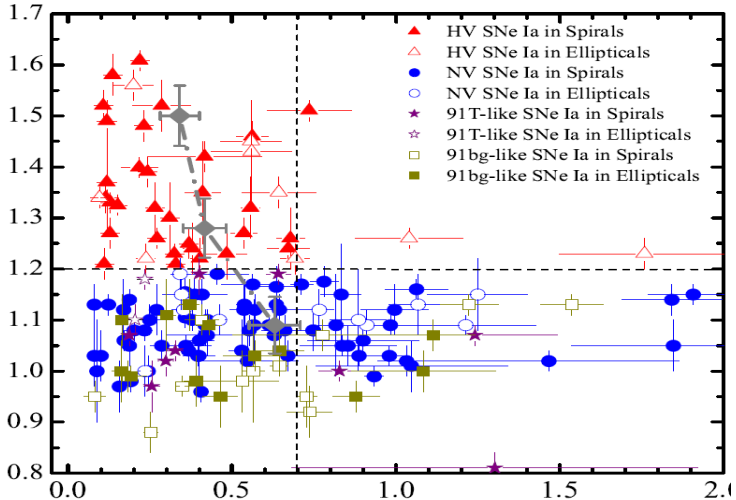

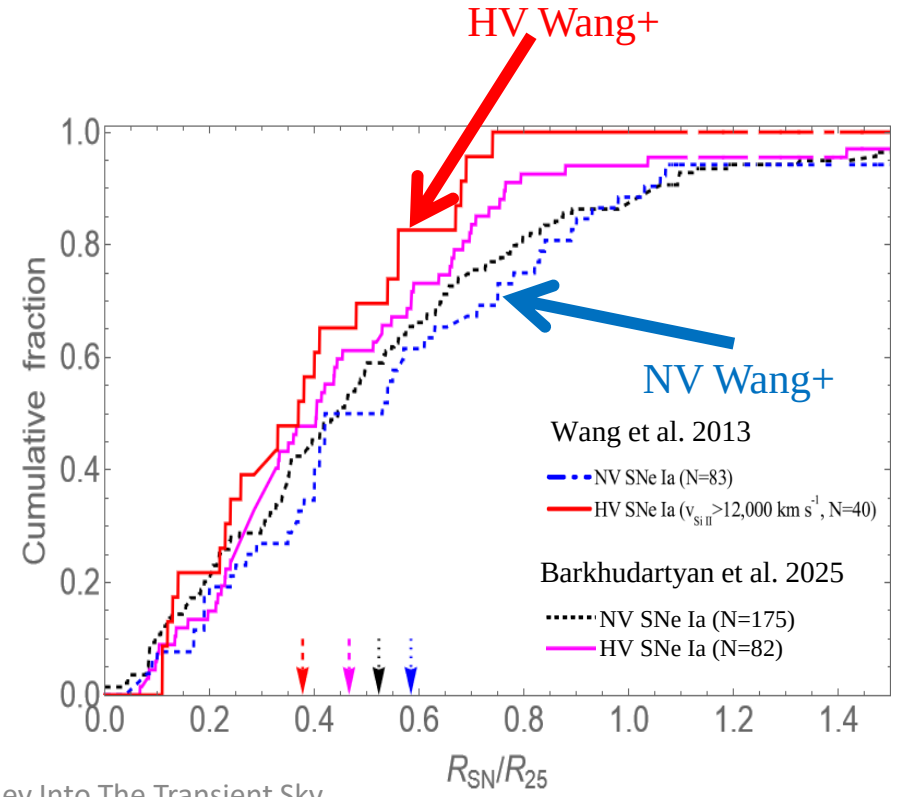

Statistically not significant result

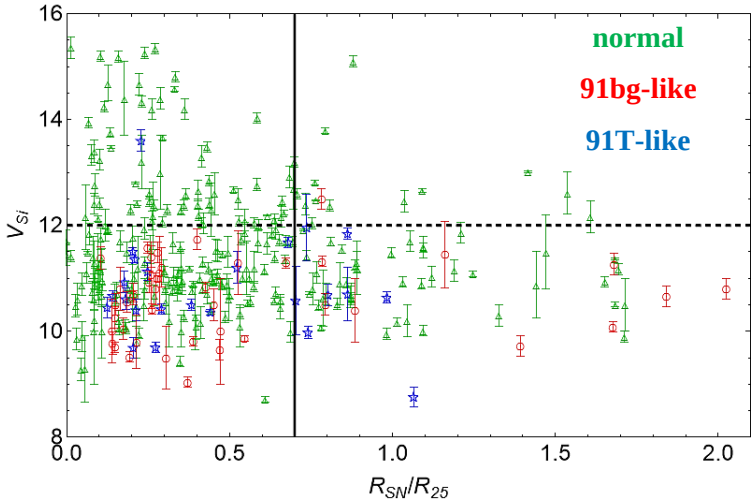

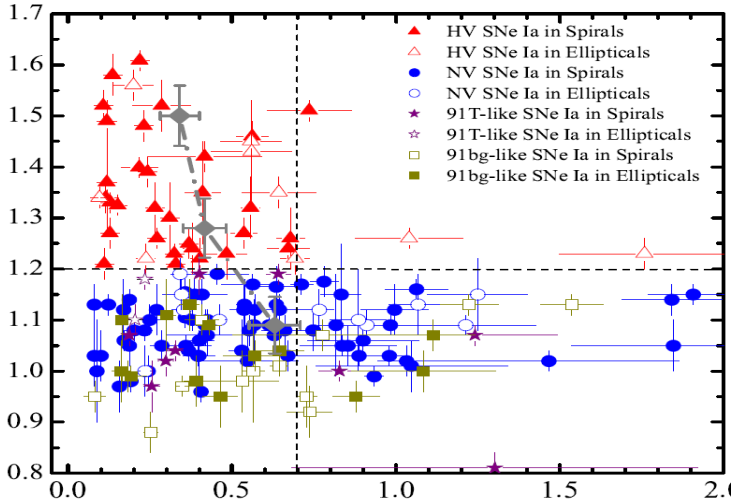

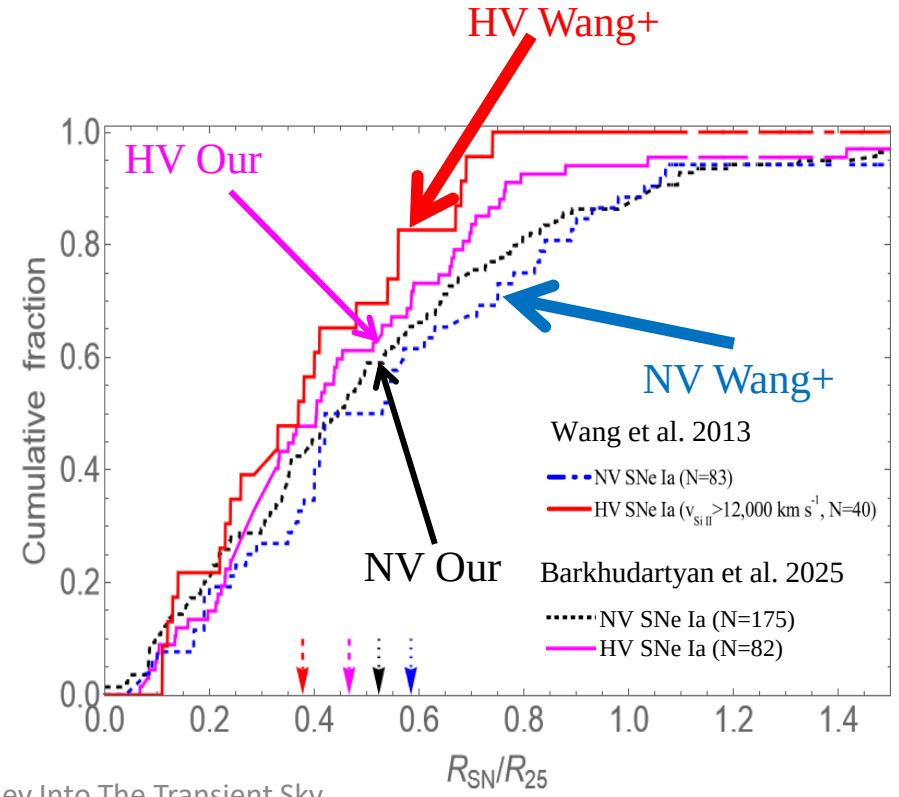

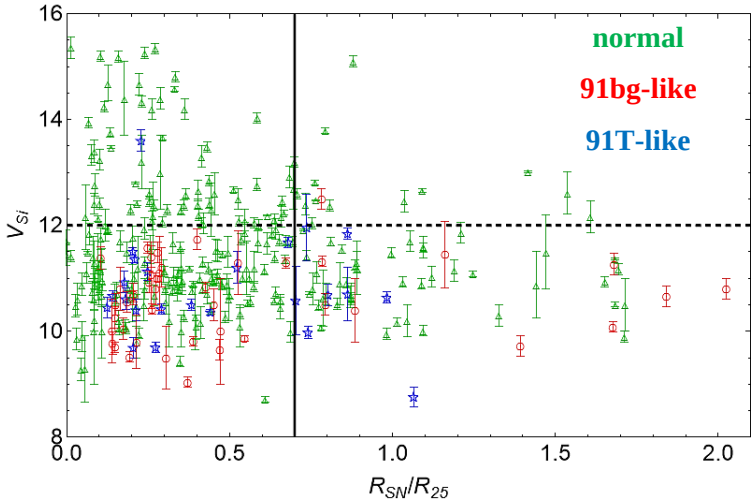

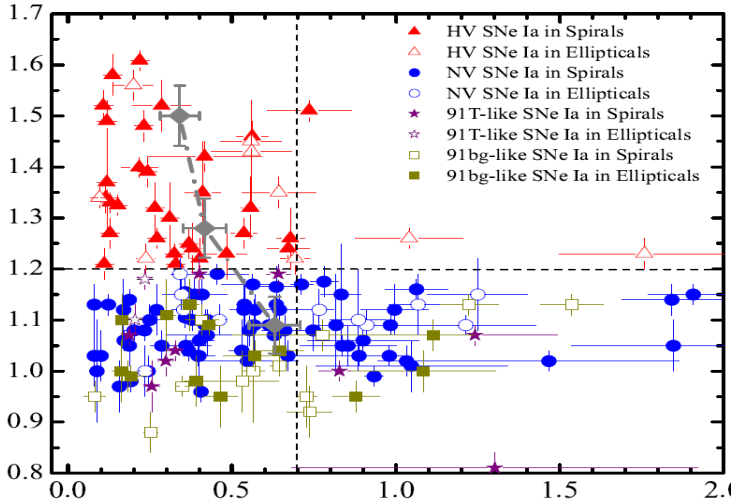

Statistically not significant result

The reason of different results

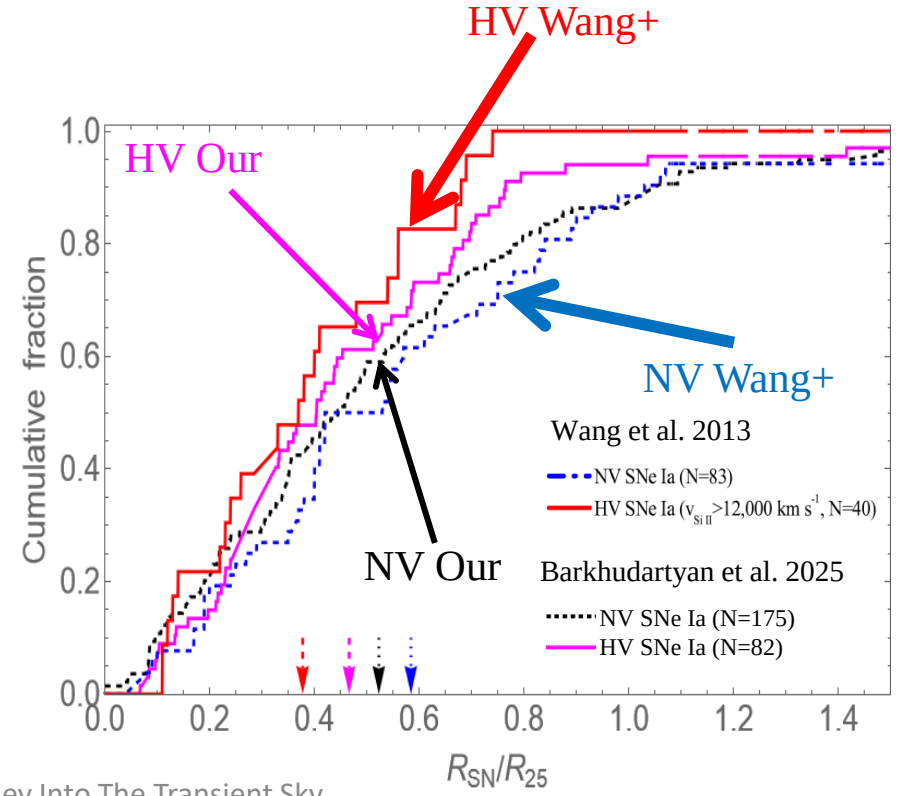

Wang sample

- Normal Ia SNe
- S0/a – Sm Spirals
- with $0° \leq i \leq 60°$ inclinations
- any galaxy exhibiting strong disturbances are excluded

Our sample

Wang sample

- Normal Ia SNe
- S0/a – Sm Spirals
- with $0° \leq i \leq 60°$ inclinations
- any galaxy exhibiting strong disturbances are excluded

Our sample

NV	***HV***
49	***22***

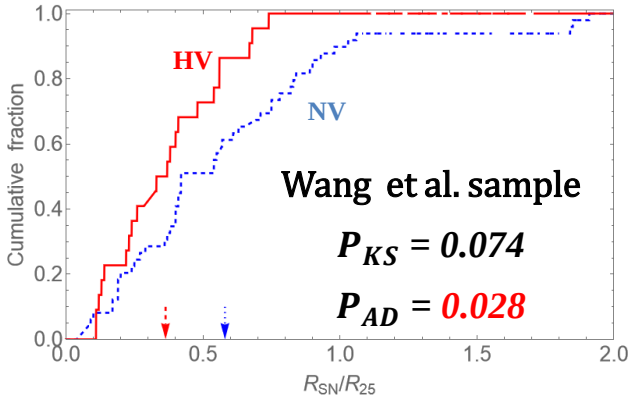

NV	***HV***
139	***67***

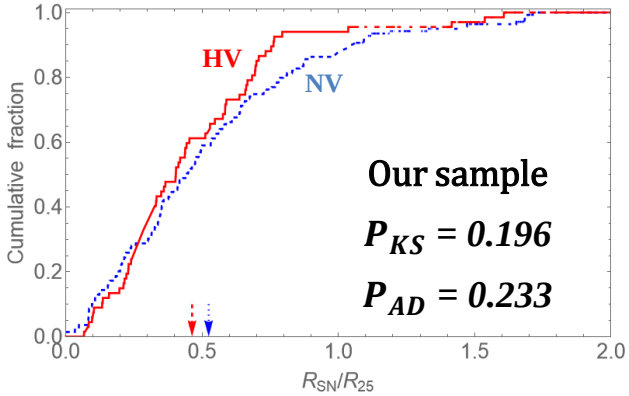

Wang sample

- Normal Ia SNe
- S0/a – Sm Spirals
- with $0° \leq i \leq 60°$ inclinations
- any galaxy exhibiting strong disturbances are excluded

Our sample

NV	***HV***
49	***22***

NV	***HV***
139	***67***

Wang's sample

Targeted ***untargeted***

surveys

Our sample

Targeted ***untargeted***

surveys

Wang sample

- Normal Ia SNe
- S0/a – Sm Spirals
- with $0° \leq i \leq 60°$ inclinations
- any galaxy exhibiting strong disturbances are excluded

Our sample

NV	*HV*
49	*22*

NV	*HV*
139	*67*

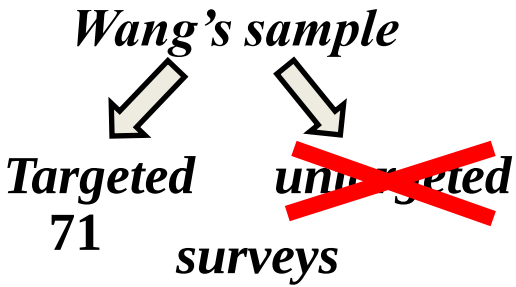

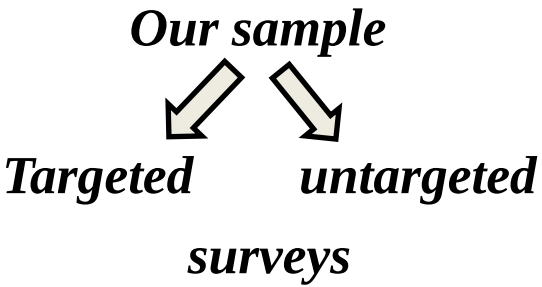

Wang sample

- Normal Ia SNe
- S0/a – Sm Spirals
- with $0° \leq i \leq 60°$ inclinations
- any galaxy exhibiting strong disturbances are excluded

Our sample

NV	*HV*
49	*22*

NV	*HV*
139	*67*

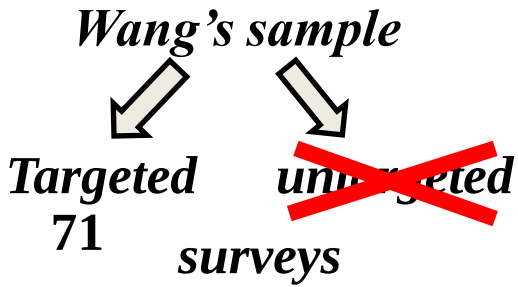

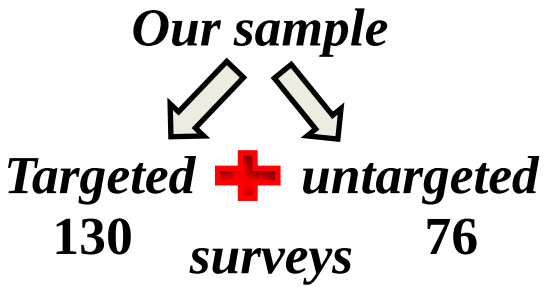

Wang sample

- Normal Ia SNe
- S0/a – Sm Spirals
- with $0° \leq i \leq 60°$ inclinations
- any galaxy exhibiting strong disturbances

NV	*HV*
49	*22*

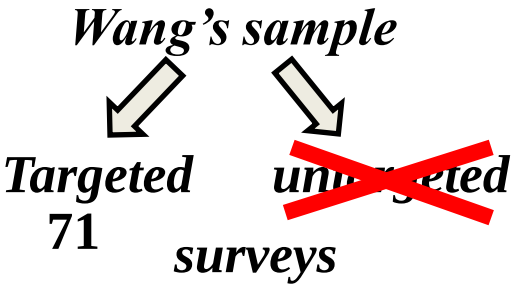

Our sample

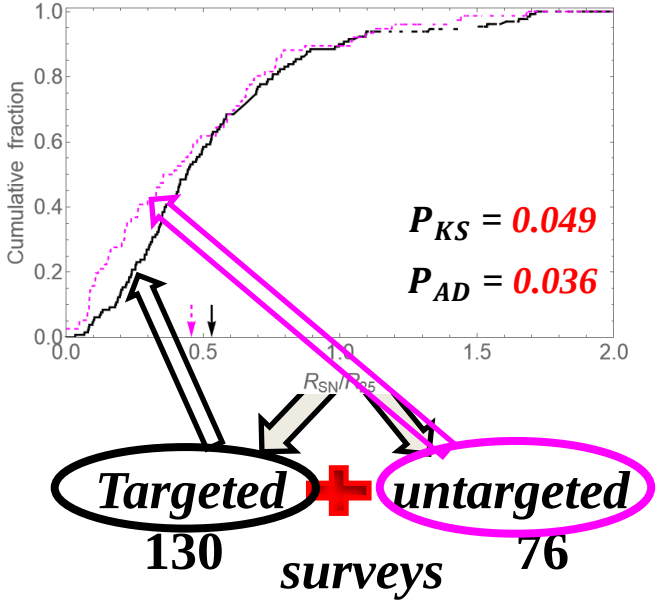

Wang sample

- Normal Ia SNe
- S0/a – Sm Spirals
- with $0° \leq i \leq 60°$ inclinations
- any galaxy exhibiting strong disturbances

NV	*HV*
49	*22*

Our sample

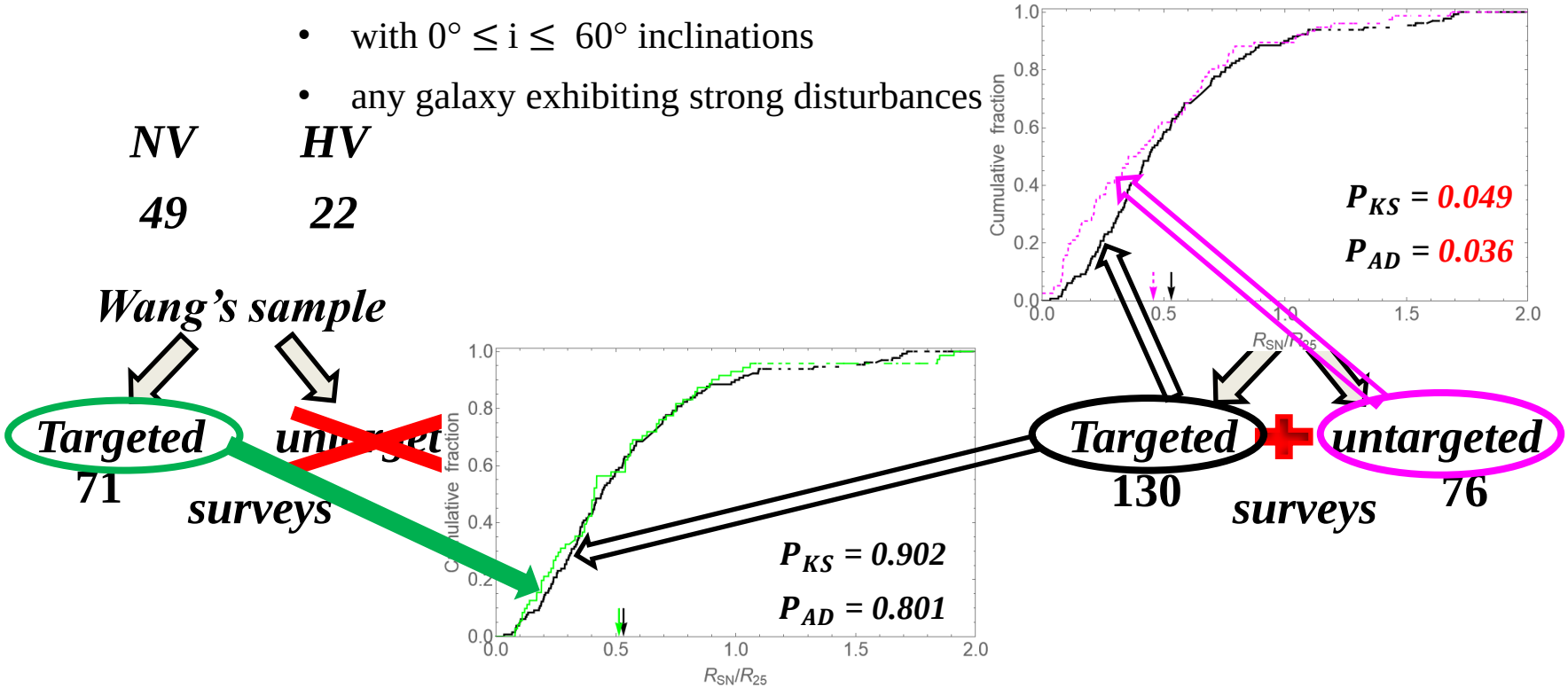

Wang sample

- Normal Ia SNe
- S0/a – Sm Spirals
- with $0° \leq i \leq 60°$ inclinations
- any galaxy exhibiting strong disturbances

NV	*HV*
49	*22*

Our sample

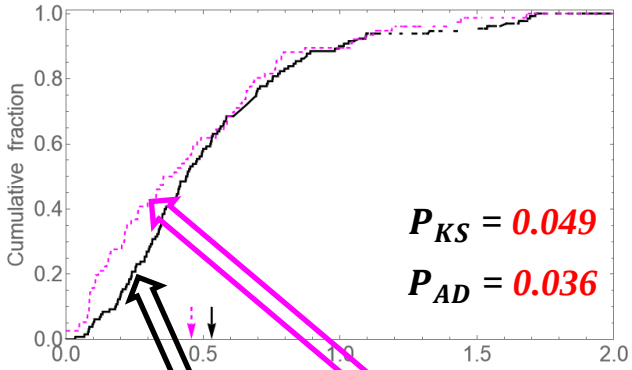

Wang's sample

Targeted

71

surveys

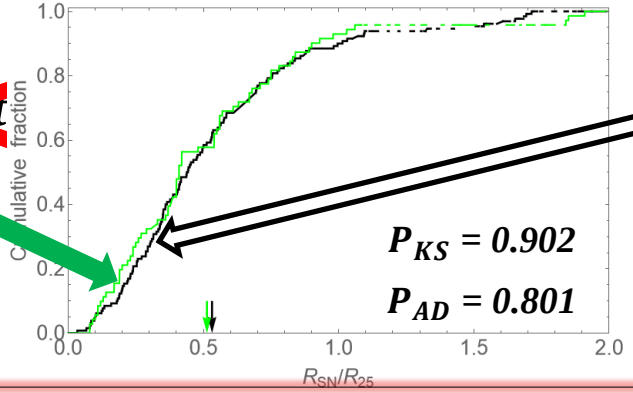

Targeted

130

surveys

untargeted

76

The targeted sample is probably biased

Wang sample

- Normal Ia SNe
- S0/a – Sm Spirals
- with $0° \leq i \leq 60°$ inclinations
- any galaxy exhibiting strong disturbances

NV	*HV*
49	*22*

Wang's sample

Targeted **71** ***surveys***

~~***untargeted***~~

Our sample

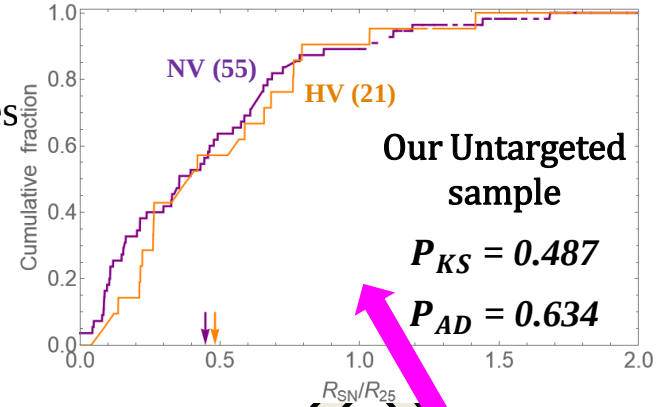

Targeted **130** ***surveys*** ***untargeted*** **76**

Wang sample

- Normal Ia SNe
- S0/a – Sm Spirals
- with $0° \leq i \leq 60°$ inclinations
- any galaxy exhibiting strong disturbances

Our sample

NV ***HV***

49 ***22***

Wang's samp

Targeted ***un***

71

surveys

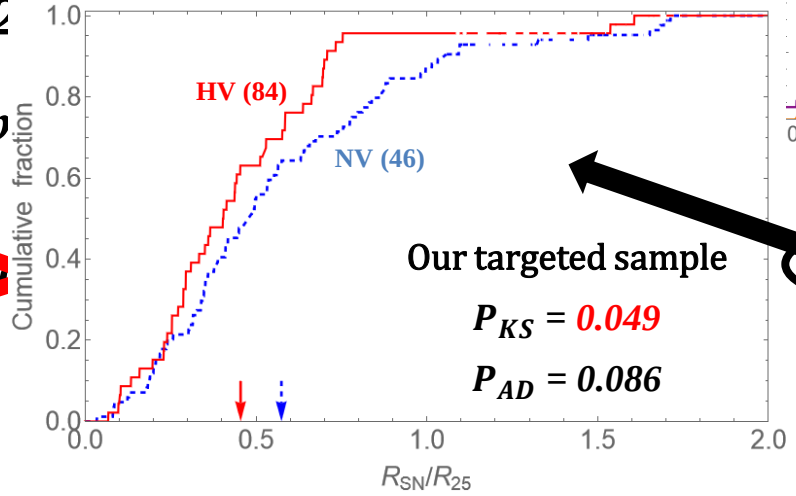

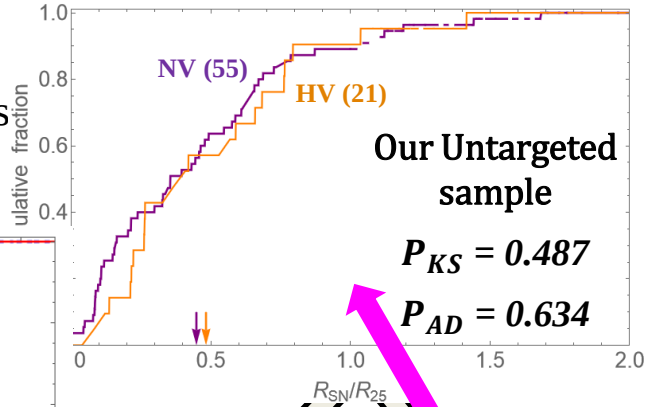

Targeted ***untargeted***

130 ***surveys*** **76**

Wang sample

- Normal Ia SNe
- S0/a – Sm Spirals
- with $0° \leq i \leq 60°$ inclinations
- any galaxy exhibiting strong disturbances

NV ***HV***

49 ***22***

Wang's samp

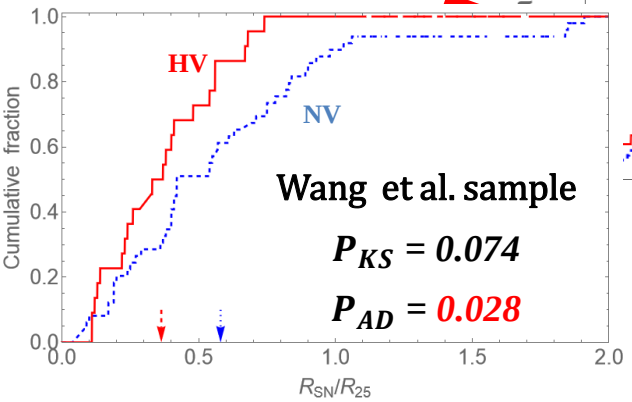

Wang et al. sample

$P_{KS} = 0.074$

$P_{AD} = 0.028$

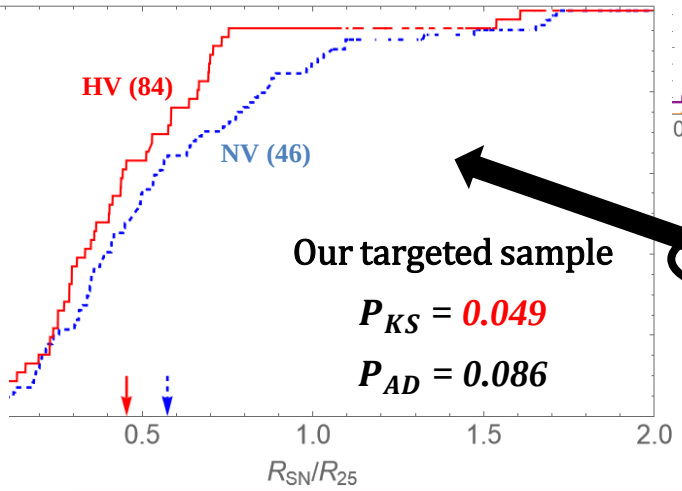

Our targeted sample

$P_{KS} = 0.049$

$P_{AD} = 0.086$

Our sample

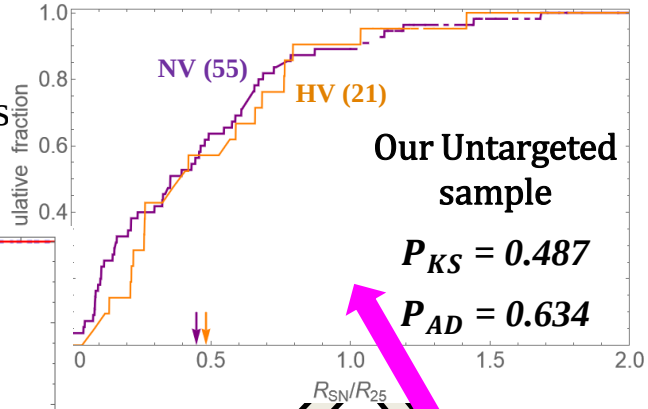

Our Untargeted sample

$P_{KS} = 0.487$

$P_{AD} = 0.634$

Targeted + ***untargeted***

130 ***surveys*** **76**

This result is due to a targeted biased sample.

Si II λ6355 velocities, plotted against the stellar galaxy masses of the volume-limited ZTF DR2 SN Ia sample for 477 SNe Ia spectra with a phase range of -5 d $\leq t_0 \leq 5$ d.

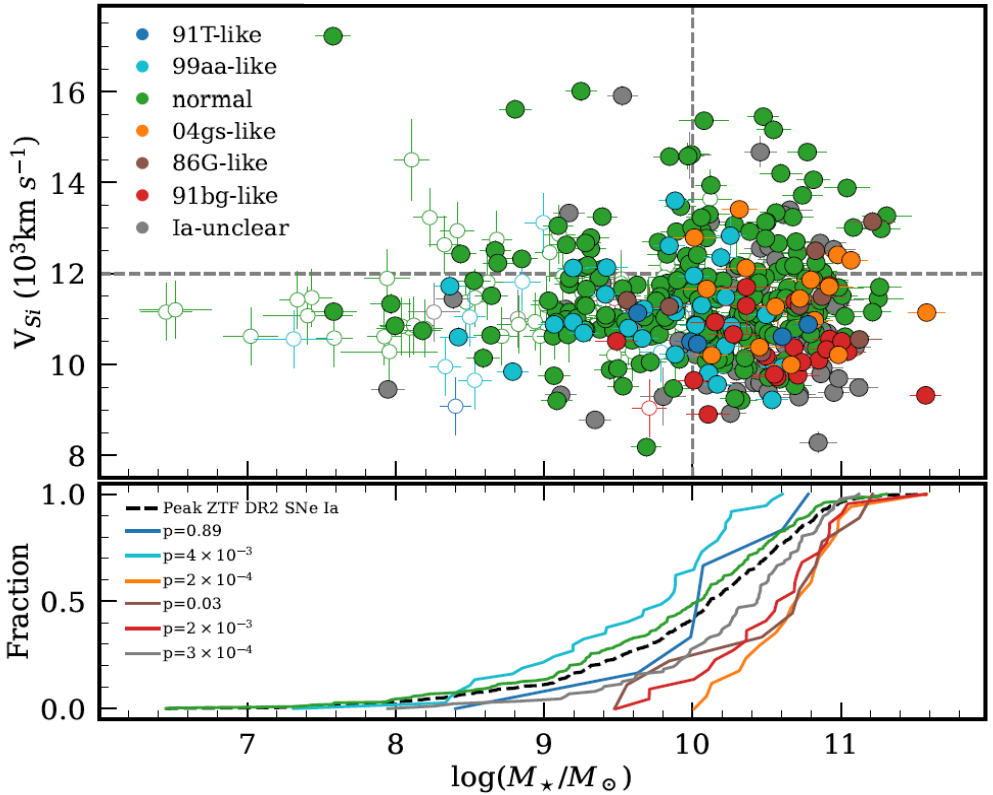

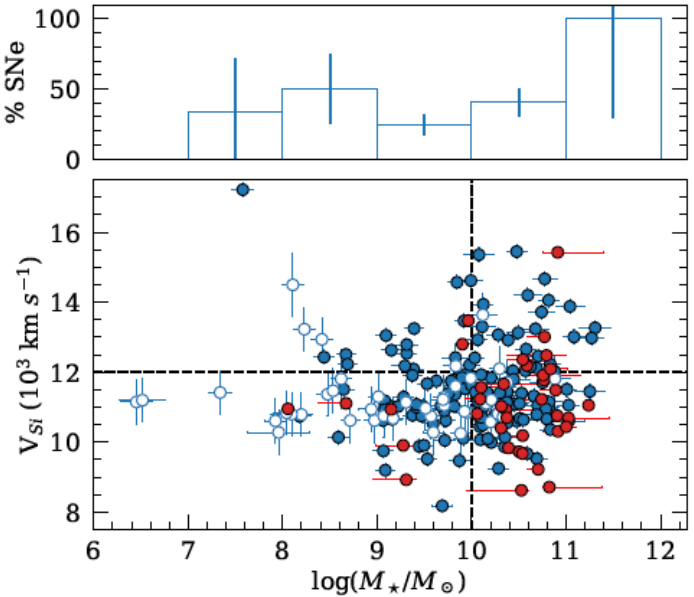

Burgaz et al. 2025

Si II λ6355 velocities, plotted against the stellar galaxy masses of the volume-limited ZTF DR2 SN Ia sample for 477 SNe Ia spectra with a phase range of -5 d $\leq t_0 \leq 5$ d.

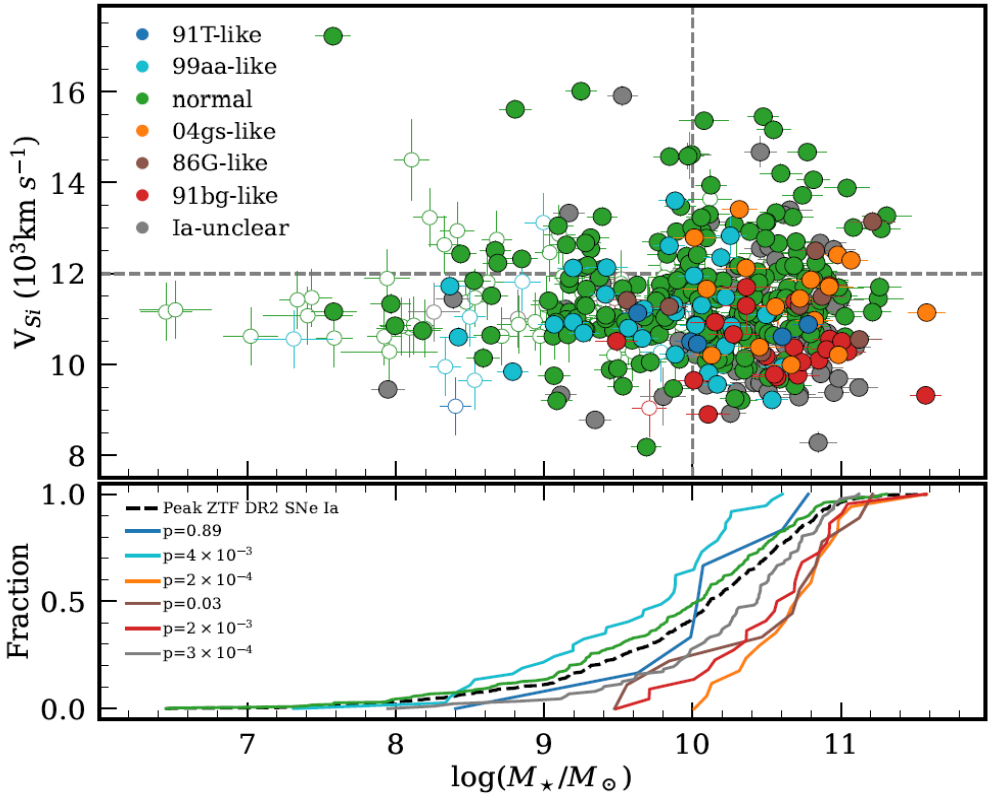

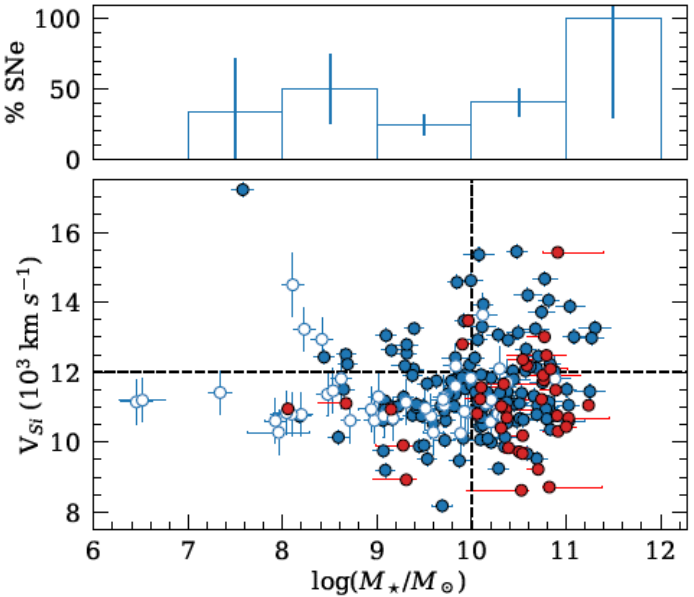

Burgaz et al. 2025

Statistically <u>not</u> significant result

CONCLUSIONS

NV SNe **vs** **HV SNe**

CONCLUSIONS

NV SNe **vs** **HV SNe**

NO GALACTOCENTRIC DISTRIBUTION DIFFERENCE

Our Result

CONCLUSIONS

NV SNe **vs** **HV SNe**

NO GALACTOCENTRIC DISTRIBUTION DIFFERENCE

Our Result

NO MASS DIFFERENCE

Result of Burgaz et al. 2025

CONCLUSIONS

NV SNe **vs** **HV SNe**

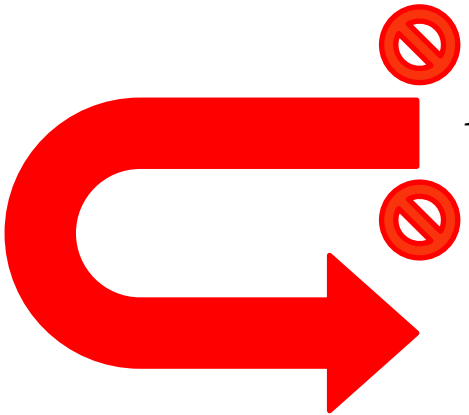

NO GALACTOCENTRIC DISTRIBUTION DIFFERENCE

Our Result

NO MASS DIFFERENCE

Result of Burgaz et al. 2025

NO PROGENITORS' METALLICITY (AGE) DIFFERENCE

CONCLUSIONS

NV SNe **vs** **HV SNe**

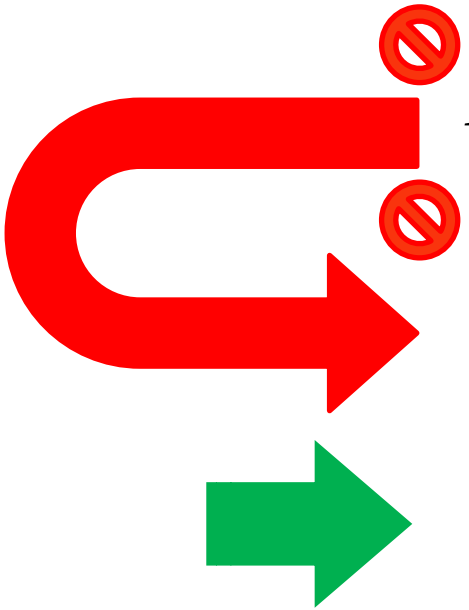

NO GALACTOCENTRIC DISTRIBUTION DIFFERENCE

NO MASS DIFFERENCE

NO PROGENITORS' METALLICITY (AGE) DIFFERENCE

SAME PARENT POPULATION

Our Result

Result of Burgaz et al. 2025

CONCLUSIONS

NV SNe **vs** **HV SNe**

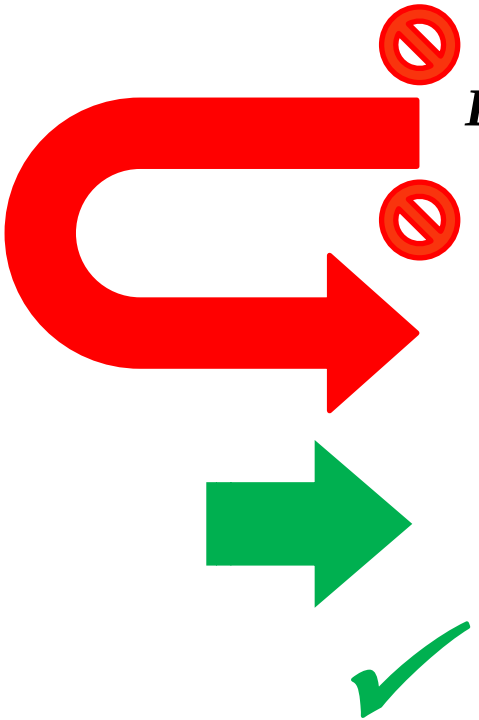

NO GALACTOCENTRIC DISTRIBUTION DIFFERENCE

Our Result

NO MASS DIFFERENCE

Result of Burgaz et al. 2025

NO PROGENITORS' METALLICITY (AGE) DIFFERENCE

SAME PARENT POPULATION

ASYMETRIC EXPLOSION

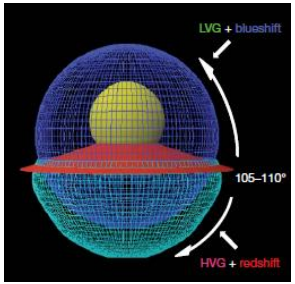

Acknowledgements.

The research was supported by the Higher Education and
Science Committee of MESCS RA (Research project 24LCG–1C021).

Thank You